Editor:
Nisit Kittipongpatana,
Chiang Mai University, Thailand

Article history:
Received: May 30, 2022;
Revised: August 18, 2022;
Accepted: August 29, 2022;
https://doi.org/10.12982/CMUJNS.2022.060

Corresponding author:
Unang Supratman,
E-mail:unang.supratman@unpad.ac.id

Research article

Sinapyl alcohols analogues from the stembark of *Zanthoxylum rhetsa* (Roxb.) DC and their cytotoxic activity against MCF-7 breast cancer cell line

Ruchiyat[1,2], Tati Herlina[1], Iqbal Musthapa[2,3], and Unang Supratman[1,4,*]

1 Department of Chemistry, Faculty of Mathematics and Natural Sciences, Universitas Padjadjaran, Jatinangor 45363, Sumedang, Indonesia.
2 Department of Chemistry, Faculty of Mathematics and Natural Sciences, Universitas Garut, Garut, 44111, Indonesia.
3 Department of Chemistry, Universitas Pendidikan Indonesia, Jl. Dr. Setiabudhi Bandung, 40141, Indonesia.
4 Central Laboratory, Universitas Padjadjaran, Jatinangor 45363, Sumedang, Indonesia.

Abstract Three sinapyl alcohol analogues, 4-*O*-[(*2E*)-3,7,7-Trimethyl-2,6-octadiene] **(1)**, 4-*O*-[(*2E*)-3,7-Dimethyl-2,7-octadiene-6-ol] **(2)** and 4-*O*-[(*2E*)(*5E*)-3,7,7-Trimethyl-2,5-octadiene-7-ol] **(3)** have been isolated from the stem bark of *Zanthoxylum rhetsa* (Roxb.) DC (Rutaceae). The chemical structures of compounds **1-3** were determined based on spectroscopic data including one and two-dimensional NMR, and mass spectroscopy. Cytotoxic activity against MCF-7 breast cancer cell lines was tested *in vitro* using these sinapyl alcohols. Among the isolated compounds 1, showed the strongest activity with an IC_{50} value of 54.18 µg/mL, suggesting that the presence of a *gem*-dimethyl and hydroxyl groups play important role for cytotoxic activity.

Keywords: Cytotoxic activity, MCF-7 cell lines, Rutaceae, sinapyl alcohol, *Zanthoxylum rhetsa* (Roxb.) DC.

Funding:
The authors are grateful to the Ministry of Research, Technology and Higher Education of Republic Indonesia for the Research Grant for Doctor Thesis, 2020 by Tati Herlina and Universitas Padjadjaran, through the Academic Leadership Grant (No: 1959/UN6.3.1/PT.00/2022 by Unang Supratman).

Citation: Ruchiyat, Herlina, T., Musthapa, I., and Supratman, U. 2022. Sinapyl alcohols analogues from the stembark of *Zanthoxylum rhetsa* (Roxb.) DC and their cytotoxic activity against MCF-7 breast cancer cell line. CMUJ. Nat. Sci. 21(4): e2022060.

INTRODUCTION

As C6-C3 building blocks, L-phenylalanine and L-tyrosine provide sinapyl alcohols as secondary metabolites. The aromatic ring of these molecules has two methoxy groups, whereas coniferyl alcohol only has one group (Dewick, 2009). The cytotoxic and anticancer properties of sinapyl alcohols make them an extremely useful class of compound (Zhao et al., 2002; Zou et al., 2005).

Sinapyl alcohol is widely distributed in various plants, especially dicotyledonous species (Dewick, 2009). Additionally, *Zanthoxylum rhetsa* from the Rutaceae family contains these compounds (Ahsan et al., 2000). The plant is a tall, deciduous tree known as "Panggal buaya" in Indonesia. In Indian tribes, this plant treats many infirmities like diabetes, inflammation, rheumatism, toothache, and diarrhea (Santhanam et al., 2016). The methanol extract of the seed and root showed antioxidant and antibacterial activity (Hayat and Vandna, 2018; Zohora et al., 2019). The stem bark showed antinociceptive and antidiarrheal activities (Rahman et al., 2002). The stem extract showed significant anti-inflammatory activity (Parthiban et al., 2017). Previous phytochemical studies showed the presence of alkaloids, lignans, flavonoids, glycosides, saponin, tannins and terpenoids (Kyaw et al., 2020; Mallya and Bhitre, 2020). Other secondary metabolites in the *Z. rhetsa* bark are sinapyl alcohol (Ahsan et al., 2000).

As part of a continuing search for pharmacologically active compounds on Indonesian Rutaceae plants, three sinapyl alcohol derivatives **(1-3)** were isolated from the stembark of *Z. rhetsa*. In this paper, the isolation and structural identification of a sinapyl alcohols **1-3** as well as the cytotoxic activity against breast cancer MCF-7 cell lines were reported.

MATERIALS AND METHODS

General experimental procedures

IR spectra were measured on Thermo Scientific™ Nicolet™ Summit FTIR Spectrometer with DTGS KBr detector and generated with Thermo Scientific™ OMNIC™ Paradigm Software (Thermo Fisher Scientific, Madison, WI, USA). Furthermore, UV spectra were recorded on TECAN Infinite M200 pro (Männedorf Switzerland) with methanol as a solvent. NMR spectra were measured by JEOL JNM-ECZ500R/S1 spectrometer (Tokyo, Japan) at 500 MHz for ^{1}H, 125 MHz for ^{13}C, and TMS as an internal standard, while mass spectra were calculated by Waters QTOF-HRTOFMS-XEVotm mass spectrometer (Waters, Milford, MA, USA). Column chromatography was conducted on silica gel 60 (70-230 and 230-400 mesh, Merck, Darmstadt, Germany). Thin-layer chromatography was carried out on silica gel 60 GF_{254} (Merck, 0.25 mm), and spots were detected under ultraviolet light of wavelength 254 nm before spraying with 10% sulfuric acid in ethanol.

Materials

The stem bark of *Z. rhetsa* (Roxb) DC was collected in September 2018 at Bogor Botanical Garden, Bogor, Indonesia, and identified by the Bogoriense Herbarium staff. A voucher specimen (No. B-816) was deposited in the Bogoriense Herbarium.

Extraction and Isolation

Air-dried stem bark of *Z. rhetsa* (Roxb) DC (5.5 kg) was powdered and extracted with methanol (36 L) at room temperature for 9 days. First, the methanol extract was evaporated under reduced pressure to yield a 593.40 g residue of the concentrated extract. This residue was dissolved in water and partitioned successively with 15L each of *n*-hexane, dichloromethane, and *n*-butanol. The evaporation of these extracts resulted in 87.90 g, 73.30 g, and 121.50 g of *n*-hexane, dichloromethane, and *n*-butanol, respectively.

Vacuum Liquid Chromatography (VLC) on silica gel G60 with *n*-hexane-ethyl acetate-methanol containing 10% increasing polarity was used to separate the dichloromethane extract of 73.30 g into five fractions of A-E. The B fraction of 14.20 g was further separated by VLC on silica gel G_{60} with *n*-hexane-ethyl acetate containing 10% ethyl acetate into five subfractions of B1-B5. Furthermore, B4 subfraction of 180 mg separated by column chromatography on octa decyl silane with a gradient solvent of MeCN-H_2O (10:0 – 2:8) yielded compound **1** of 14.5 mg. Finally, the B5 subfraction of 220 mg was separated by preparative thin layer chromatography (PTLC) on silica gel GF_{254} with *n*-hexane-dichloromethane-acetone (7.5:0.5:2) as a solvent system to yield compounds **2** and **3** of 5 mg and 6 mg.

Cytotoxic activity assay

Cell viability was assessed with Presto Blue reagent (Thermo Fisher Scientific, Uppsala, Sweden) to evaluate various resazurin-based cell types' viability rapidly and quantitatively using live-cell reduction capabilities. The cytosol of healthy cells kept at a relatively constant pressure. The reduction of resazurin (blue) serve as a cell viability indicator by utilizing absorbance or fluorescence outputs to diminish resorufin (purple). The conversion is proportional to the number of metabolically active cells. MCF-7 cell lines were extracted and counted at 70% confluence before diluting with complete culture RPMI media. The cells were then transferred into 96 well-plates with 170,000 cells/well. After overnight growth, they were treated with increasing concentrations of compounds **1-3** (3.91, 7.81, 15.63, 31.25, 62.50, 125, 250, 5,000 ppm) with co-solvent 2% (v/v) DMSO in PBS. Furthermore, Cisplatin was used as the positive control, and the entire samples were incubated at 37°C in a 5% CO_2 incubator for 24 hours. A 10 µL PrestoBlue reagent immediately replaced the medium in a 90 µL RPMI medium. The plates were incubated for 1-2 hours until resorufin was formed, allowing the color to change from blue to purple. The absorbance was measured at 570 nm using a microplate reader. IC_{50} values were taken from the plotted graph of percentage live cells compared to control (%), receiving DMSO, versus the tested concentration of compounds (µg/mL). The IC_{50} values mean concentration required for 50% growth inhibition (Camarillo et al., 2014; Macana et al., 2011). PrestoBlue assay and analysis were run in duplicate and averaged.

RESULTS

4-*O*-[(*2E*)-3,7,7-Trimethyl-2,6-octadiene]-sinapyl alcohol (1). Yellow solid; IR (NaCl) ν_{max} 3391, 2932, 1581, 1503, 1453, 1239, 1115 and 955 cm^{-1}; ^{1}H-NMR ($CDCl_3$, 500 MHz): δH 6.58 (2H, s, H-2 and H-6), 6.52 (1H, d, *J*= 16.0 Hz, H-7), 6.29 (1H, dt, *J*= 5.5,16.0 Hz, H-8), 5.57 (1H, t, *J*= 6.8 H-2'), 5.08 (1H, t, *J*= 6.5, H-6'), 4.54 (2H, d, *J*= 7.0 Hz, H-1'), 4.33 (2H, d, *J*= 5.5 Hz, H-9), 2.05 (2H, q, *J*= 6.5, 3.0 Hz, H-5'), 2.00 (2H, q, *J*= 7.9 Hz, H-4'), 1.67 (3H, s, H-8'), 1.59 (3H, s, Me-9'), 1.65 (3H, s, Me-10'), 3.84 (6H, s, 3-OMe and 5-OMe), ^{13}C-NMR ($CDCl_3$, 125 MHz), see Table 1; HR-TOFMS *m/z* found 347.2216 $[M+H]^+$, (calculated for $C_{21}H_{31}O_4$, *m/z* 347.2222).

4-*O*-[(*2E*)-3,7-Dimethyl-2,7-octadiene-6-ol]-sinapyl alcohol (2). Yellow solid; IR (NaCl) ν_{max} 3386, 2932, 1581, 1502, 1455, 1239, 1127, 966 cm^{-1}; ^{1}H-NMR ($CDCl_3$, 500 MHz) δH 6.57 (1H, s, H-2 and H-6), 6.54 (1H, d, *J*= 15.5 Hz, H-7), 6.23 (1H, dt, *J*= 6.0, 15.5 Hz, H-8), 5.58 (1H, t, *J*= 8.5 Hz, H-2'), 5.32 (1H, d, *J*=12.0 Hz, H-8'b), 5.18 (1H, d, *J*=12.0 Hz, H-8'a), 4.52 (2H, t, *J*= 8.5 Hz, H-1'), 4.31 (2H, d, *J*= 6.0 Hz, H-9), 3.96 (1H, t, *J*= 7.5 Hz, H-6'), 3.83 (6H, s, 3-OMe and 5-OMe), 2.03 (2H, m, H-4'), 1.68 (3H, s, Me-9'), 1.63 (3H, s, Me-10'), 1.61 (2H, m, H-5'); ^{13}C NMR ($CDCl_3$, 125 MHz) see Table 1; HR-TOFMS *m/z* found 385.1990 $[M+Na]^+$, (calculated for $C_{21}H_{30}O_5Na$, *m/z* 385.1991).

4-*O*-[(*2E*),(*5E*)-3,7,7-Trimethyl-2,5-octadiene-7-ol]-sinapyl alcohol (3). Yellow solid; IR (NaCl) ν_{max} 3355, 2932, 1582, 1504, 1459, 1239, 1127, 963 cm^{-1}; ^{1}H-NMR ($CDCl_3$, 500 MHz) δH 6.60 (1H, s, H-2 and H-6), 6.55 (1H, d, *J*= 16.0 Hz, H-

7), 6.29 (1H, dt, *J*= 6.0, 16.0 Hz, H-8), 5.56 (1H, m, H-2'), 4.54 (2H, d, *J*= 7.0 Hz, H-1'), 4.32 (2H, d, *J*= 5.0 Hz, H-9), 2.70 (2H, d, *J*= 6.0 Hz, H-4'), 5.58 (1H, dd, *J*=6.7, 12.4 Hz, H-5'), 5.57 (1H, d, *J*=12.4 Hz, H-6'), 3.84 (6H, s, 3-OMe and 5-OMe), 1.62 (3H, s, Me-10'), 1.30 (3H, s, Me-8' and Me-9'); ^{13}C NMR ($CDCl_3$, 125 MHz) see Table 1; HR-TOFMS *m/z* found 385.2008 $[M+Na]^+$, (calculated for $C_{21}H_{30}O_5Na$, *m/z* 385.1991).

Table 1. ^{13}C-NMR data of Compounds **1-3** (125 MHz, in $CDCl_3$).

Position Carbon	Compounds		
	1 δc (mult.)	**2** δc (mult.)	**3** δc (mult.)
1	132.3 (s)	132.4 (s)	132.4 (s)
2	103.5 (d)	103.6 (d)	103.5 (d)
3	153.8 (s)	153.8 (s)	153.8 (s)
4	136.7 (s)	136.7 (s)	136.5 (s)
5	153.8 (s)	153.8 (s)	153.8 (s)
6	103.5 (d)	103.6 (d)	103.5 (d)
7	131.4 (d)	131.3 (d)	131.4 (d)
8	127.9 (d)	127.8 (d)	128.0 (d)
9	63.8 (t)	63.8 (t)	63.8 (t)
1'	69.6 (t)	69.4 (t)	69.4 (t)
2'	120.3 (d)	120.6 (d)	121.3 (d)
3'	141.5 (s)	141.1 (s)	140.2 (s)
4'	39.7 (t)	35.6 (t)	42.0 (t)
5'	26.5 (t)	32.8 (t)	124.5 (d)
6'	124.1 (d)	75.4 (d)	139.9 (d)
7'	131.7 (s)	147.5 (s)	70.8 (s)
8'	25.8 (q)	111.2 (t)	29.6 (q)
9'	17.8 (q)	17.7 (q)	29.6 (q)
10'	16.5 (q)	16.4 (q)	16.4 (q)
3-OMe	56.1 (OMe)	56.2 (OMe)	56.1 (OMe)
5-OMe	56.1 (OMe)	56.2 (OMe)	56.1 (OMe)

Table 2. Cytotoxic activity of compounds **1-3** against MCF-7 breast cancer cell lines.

Compounds	IC_{50}(µg/mL)
4-*O*-[(*2E*)-3,7,7-Trimethyl-2,6-octadiene]sinapyl alcohol **(1)**	54.2
4-*O*-[(*2E*)-3,7-Dimethyl-2,7-octadiene-6-ol]sinapyl alcohol **(2)**	92.5
4-*O*-[(*2E*)(*5E*)-3,7,7-Trimethyl-2,5-octadiene-7-ol]sinapyl alcohol **(3)**	60.2
Cisplatin*	53.0

Note: *Positive control

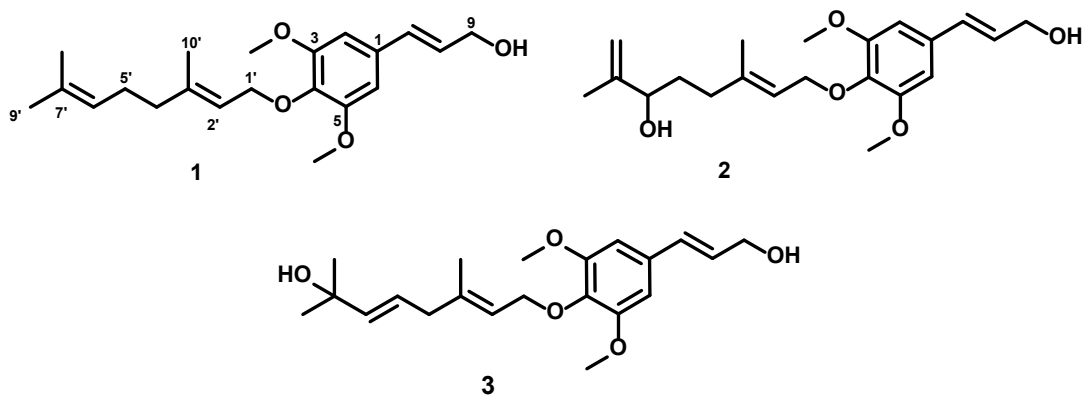

Figure 1. Structures of compounds 1-3.

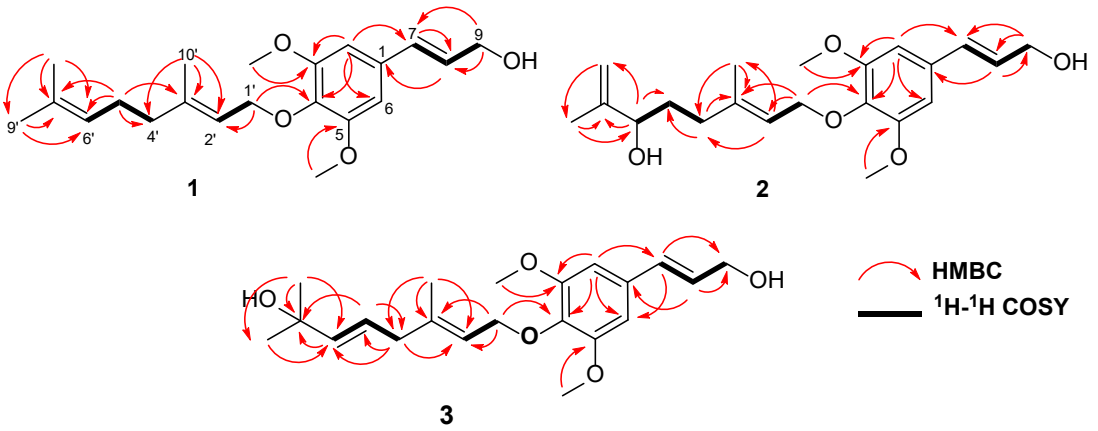

Figure 2. HMBC and ^{1}H-^{1}H COSY correlations of compounds 1-3.

DISCUSSION

The dichloromethane extract of the stem bark of *Z. rhetsa* (Roxb) DC was separated over a vacuum-liquid chromatographed (VLC) column packed with silica gel G60 by gradient elution. The VLC fraction was repeatedly subjected to reverse- and normal-phase column chromatography to yield three sinapyl alcohols, **1-3** (Figure 1).

Compound **1** was obtained as a yellow solid, and the molecular formula was identified as $C_{21}H_{30}O_4$ by HR-ESI-TOFMS. It showed $[M+H]^+$ molecular ion peak at *m/z* 347.2216, calculated for $C_{21}H_{31}O_4$, *m/z* 347.2222, and NMR data using seven degrees of unsaturation. The UV spectrum showed the absorption peak at λ_{max}, nm (log ε): 324 (4.90), 280 (4.50), and 210 (4.70), indicating the presence of phenolic compounds (Shiono et al., 2013; Sianturi et al., 2016). The IR spectrum reported hydroxyl at 3,400 cm^{-1}, aliphatic carbon at 2,932 and 2,834 cm^{-1}, conjugated double bond at 1,581 cm^{-1}, *gem*-dimethyl at 1,453 and 1,330 cm^{-1}, and ether groups of 1115 cm^{-1}. The ^{1}H-NMR spectrum exhibited the presence of three tertiary methyl protons at δH 1.67 (3H, s, Me-8'), 1.59 (3H, s, Me-9'), and 1.65 (3H, s, Me-10'), two methoxyl protons at 3.84 (6H, s, 3-OMe, and 5-OMe) and six olefinic protons at δH 6.58 (2H, s, H-2, and H-6), 6.52 (1H, d, *J*=16.0 Hz, H-7), 6.29 (1H, dt, *J*=5.5, 16.0 Hz, H-8), 5.57 (1H, t, *J*=6.8 Hz, H-2'), 5.08 (1H, t, *J*=6.5 Hz, H-6'). The large coupling constant (*J*=16.0 Hz) from olefinic protons at C-7 and C-8 indicated the *E*-configuration. Additionally, two oxygenated methylene protons at δH 4.33 (2H, d, *J*=5.5 Hz, H-9) and 4.54 (2H, d, *J*=7.0 Hz, H-1') were also observed in the ^{1}H-NMR spectrum. A total of 21 carbon resonances were observed in the ^{13}C NMR spectrum.

These were assigned by DEPT and HMQC experiments as tetra-substituted aromatic carbons at δC 132. 3 (s), 103.5 (d, 2×), 153.8 (s 2×) and 136.7 (s), six olefinic carbons at δC 141.5 (s), 131.7 (s), 131.4 (d), 127.9 (d), 124.1 (d) and 120.3 (d), two methoxy carbons at δC 56.1 (3-OMe and 5-OMe), two oxygenated methylene carbons at δC 63.8 (t) and 69.6 (t), three methyl carbons at δC 25.8 (q), 17.8 (q) and 16.5 (q), and two sp^3 methylene carbons at δC 39.7 (t) and 26.5 (t). Meanwhile, these functionalities accounted for six out of the seven degrees of unsaturation. The remaining one degree of saturation was consistent with sinapyl alcohol; analogues (Zhao et al., 1994; Gao et al., 1998; Zhao et al., 2002).

The position of the functional group in compound **1** was clarified through the ^1H-^1H COSY and HMBC experiments, and the results are shown in Figure 2. The ^1H-^1H COSY spectrum exhibited correlations in H_7-H_8-H_9, $H_{1'}$-$H_{2'}$, and $H_{4'}$-$H_{5'}$-$H_{6'}$, supporting the presence of geranyloxy sinapyl alcohol skeleton. Furthermore, the skeleton of sinapyl alcohol was determined by HMBC correlations (Figure 2) of tertiary methyl and olefinic protons. The correlations of Me-9' and Me-8' to C-7' δC 131.7), Me-10' to C-3' (δC 153.8), and C-2' (δC 120.3) as well as that oxygenated proton at C-1' (δH 4.54) to C-2' (δC 120.3) and C-4 (δC 136.7), indicated the presence of geranyloxy at C-4. Two olefinic protons at δH 6.52 and 6.29 can be coupled and correlated to C-9 (δC 63.8) and C-1 (δC 132.3), supporting the presence of sinapyl alcohol. Additionally, two methoxy protons at δC 56.1 were correlated to C-C-3 (δC 153.8), indicating methoxy's position at C-3 and C-5, respectively. Aromatic proton signals at δH 6.58 (2H, s) indicated the tetra-substituted benzene ring. The detailed examination of the NMR spectral data and comparison with those reported for 3,5-Dimethoxy-4-geranylcinnamylalcohol (Zhao et al., 1994; Gao et al., 1998; Ahsan et al., 2000) showed that the structures are very similar. Therefore, compound **1** was identified as 3,5-Dimethoxy-4-geranylcinnamylalcohol or 4-*O*-[(*2E*)-3,7,7-trimethyl-2,6-octadiene]sinapyl alcohol and was isolated for the first time in the *Zanthoxylum rhetsa* (Roxb.) DC.

Compound **2** was obtained as a yellow solid with a molecular formula of $C_{21}H_{30}O_5$, based on HR-ESI-TOFMS analysis. This evaluation elucidated a $[M+H]^+$ ion peak at *m/z* 385.1991 (calcd. for $C_{21}H_{30}O_5$, *m/z* 385.1990) hence seven degrees of unsaturation are required. The IR spectrum and NMR data observed were highly similar to those of compound **1**. However, the difference was identified in the absence of one of the olefinic and methyl protons and also the appearance of a newly oxygenated proton [δH 3.96 (1H, d, *J*=7.5 Hz), δC 75.4)] and methylene sp^2 protons [δH 5.18 (1H, d, *J*=12.0 Hz), 5.32 (1H, d, *J*=12.0 Hz), δC 111.2)]. These observations suggest compound **2** to be a hydroxy derivative of 1, which is further supported by the HMBC correlations from δH 3.96 (H-6') to 147.5 (C-7') and from δH 5.18 to 147.5 (C-7'), indicating the position of hydroxyl and methylene at C-6' and C-7', respectively. These observations with the similarity of spectral data and physicochemical properties between **2** and previously reported 4-*O*-[6-hydroxy-7(9)-dehydro-6,7-dihydrogeranyl]-coferyl alcohol, isolated from the root of *Ligularia duciformis* (Gao et al., 1998), identified **2** as 4-*O*-[6-hydroxy-7(9)-dehydro-6,7-dihydrogeranyl]-coferyl alcohol, which was also isolated from *Zanthoxylum rhetsa* (Roxb.) DC for the first time.

Compound **3** was isolated as a yellow solid with the molecular formula established as $C_{21}H_{30}O_5$. This estimation was based on ion peak at *m/z* 385.2008 $[M+Na]^+$ (calcd. for $C_{21}H_{30}O_5Na$, *m/z* 385.1991), observed in the HR-ESI-TOFMS spectrum, indicating the presence of seven degrees of unsaturation. Furthermore, the IR and 1D NMR data suggest analogous features with 1. The differences were observed in the absence of the olefinic proton and the presence of a new trans-olefinic proton [δH 5.58 (1H, dd, *J*=6.7, 12.4 Hz), δH 5.57 (1H, d, *J*=12.4 Hz), δC 124.5 and 139.9] and oxygenated sp^3 carbon at δC 70.8. To clarify the position of the new functional group, ^1H-^1H COSY and HMBC experiments were conducted, and the results are shown in Figure 2. An olefinic proton at δH 5.57 was correlated to oxygenated carbon at δC 70.8 and olefinic carbon at δC 124.5. In contrast, methyl proton at δH 29.6 was also correlated to oxygenated carbon at δC 70.8, indicating that C-8', C-7', and C-6' formed α, β unsaturated tertiary alcohol. A comparison of the NMR data of 3 to those of 4-*O*-[7-hyroxy-5,6E-dehydro-6,7-dihydrogeranyl]-coniferyl

alcohol (Gao et al., 1998) showed high similarity. Consequently, compound **3** was identified as a 4-*O*-[7-hyroxy-5,6E-dehydro-6,7-dihydrogeranyl]-coniferyl alcohol, which is even isolated for the first time in *Zanthoxylum rhetsa* (Roxb.) DC.

The cytotoxic activity of the isolated compounds 1-3 was evaluated against the MCF-7 breast cancer cell lines according to a method described previously (Xu et al., 2015; Supratman et al., 2020; Naini et al., 2022). Cisplatin of 53 µg/mL was used as the positive control, as shown in Table 2. Among all sinapyl alcohols, compounds **(1)** and **(2)** showed the strongest and lowest cytotoxic activity with an IC_{50} value of 54.18 µg/mL and 92.51 g/mL, respectively.

These results indicated that cytotoxic activity of sinapyl alcohol compounds are affected by the presence of *gem*-dimethyl and hydroxyl groups.

CONCLUSION

Three known sinapyl alcohol compounds, 4-*O*-[(*2E*)-3,7,7-Trimethyl-2,6-octadiene]sinapyl alcohol **(1)**, 4-*O*-[(*2E*)-3,7-Dimethyl-2,7-octadiene-6-ol]sinapyl alcohol **(2)**, and 4-*O*-[(*2E*)(5E)-3,7,7-Trimethyl-2,5-octadiene-7-ol]sinapyl alcohol **(3)** were isolated from dichloromethane extract of the stem bark of *Z. rhetsa* (Roxb.) DC. Compounds **(2**) and **(3)** were isolated from the genus *Zanthoxylum* for the first time. Furthermore, the cytotoxic activity of compounds **1-3** against MCF-7 breast cancer cell lines was evaluated and indicated the present of *gem*-dimethyl and hydroxyl groups play important role for cytotoxic activity.

ACKNOWLEDGMENTS

The authors are grateful to Sofa Fajriah at the Research Center for Chemistry, National Innovative and Research Council, Indonesia for NMR measurements. Authors gratefully also to Universitas Padjadjaran (Academic Leadership Grant, number, 1959/UN6.3.1/PT.00/2022 by Unang Supratman).

AUTHOR CONTRIBUTIONS

Unang Supratman and Tati Herlina assisted in conducting the experiments, performed the spectral analysis, and wrote the manuscript. Ruchiyat and Iqbal Mustapha designed and conducted all experiments, as well as wrote the manuscript. All authors have read and approved the final manuscript.

CONFLICT OF INTEREST

The authors declare that they hold no competing interests.

REFERENCES

Ahsan, M., Zaman, T. A., Hasan, C.M., Ito, C., and Nazrul Islam, S.K. 2000. Constituents and cytotoxicity of *Zanthoxylum rhesta* stem bark. Fitoterapia. 71: 697-700.

Camarillo, I.G., Xiao, F., Madhivanan, S., Salameh, T., Nichols, M., Reece, L.M., Leary, J.F., Otto, K.J., Natarajan, A., Ramesh, A., and Sundararajan, R. 2014. "Low and high voltage electrochemotherapy for breast cancer: An *in vitro* model study" in Electroporation-Based Therapies for Cancer. Eds. Sundararajan. R. Woodhead Publishing. Cambridge. United Kingdom.

Dewick, P.M. 2009. Medicinal natural products: A biosynthetic approach, 3rd Edition. John Wiley & Sons. Ltd.

Gao, K., Wang, W.S., and Jia, Z.J. 1998. Coniferyl and sinapyl alcohol derivatives from *Ligularia duciformis*. Phytochemistry. 47: 269-272.

Hayat, M. and Vandna, K. 2018. A review on medicinal properties of *Zanthoxylum armatum* DC. Research Journal of Pharmacy and Technology. 11: 2131 2138.

Kyaw, C.M., Lae, K.Z.W., and Ngwe, D.H. 2020. Investigation of phytochemical constituents and some biological activities of the spine of *Zanthoxylum rhetsa* (Roxb.) Dc.(Ka-Thit-Phu). Journal of the Myanmar Academy of Arts and Science. XVIII (1B): 103-116.

Machana, S., Weerapreeyakul, N., Barusrux, S., Nonpunya, A., Sripanidkulchai, B., and Thitimetharoch, T. 2011. Cytotoxic and apoptotic effect of six herbal plants against the human hepatocarcinoma (HepG2) cell line. Chinese Medicine. 6 : 1–8.

Mallya, R. and Bhitre, M.J. 2020. Cytotoxic activity and initiation of apoptosis via intrinsic pathway in jurkat cells by leaf extract of *Zanthoxylum rhetsa* DC. Nutrition and Cancer. 73:1768-1779.

Naini, A., Hidayat, A.T., Mayanti, T., Nurlelasari, Harneti, D., Maharani, R., Safari, A., Shiono, Y., Farabi, K., Lesmana R., and Supratman, U. 2022. Cytotoxic sesquiterpenoids from *Dysoxylum parasiticum* (Osbeck) Kosterm. stem bark. Phytochemistry Letters. 47: 102–106.

Parthiban, S., Kumar, K.G., Boopathi, T., Sangeetha, G., Kokila, T., and Devan, V.S. 2017. *In vitro* anti inflammatory activity of stem of *Zanthoxylum rhetsa* (Roxb.) DC. World Journal of Pharmaceutical Research. 6: 591-600.

Rahman, M. T., Alimuzzaman, M., Ahmad, S., Chowdhury, A. A. 2002. Antinociceptive and antidiarrhoeal activity of *Zanthoxylum rhetsa*, Fitoterapia. 73: 340-342.

Santhanam, R.K., Ahmad, S., Abas, F., Safinar Ismail, I., Rukayadi, Y., Tayyab Akhtar, M., and Shaari, K. 2016. Bioactive constituents of *Zanthoxylum rhetsa* bark and its cytotoxic potential against B16-F10 melanoma cancer and normal human dermal fibroblast (HDF) cell lines. Molecules. 21: 652.

Shiono, Y., Sasaki, T., Shibuya, F., Yasuda, Y., Koseki, T., and Supratman, U. 2013. Isolation of a phomoxanthone A derivative, a new metabolite of tetrahydroxanthone, from a *Phomopsis* sp. Isolated from the mangrove, *Rhizhopora mucronata*. Natural Product Communications. 8: 1735-1737.

Sianturi, J., Harneti, D., Darwati, Mayanti, T., Supratman, U., and Awang, K. 2016. A new (-)-5′,6-dimethoxyisolariciresinol-(3″,4″-dimethoxy)-3α-O-β-D-glucopyranosides from the bark of *Aglaia eximia* (Meliaceae). Natural Product Research. 30: 2204–2208.

Supratman, U., Katja, D.G., Salam, S., Naibaho, W., Fajar, M., Nurlelasari, Nafiah, M.A., Harneti, D., Maharani, R., Hidayat, A.T., Lesmana, R., and Shiono, Y. 2020. New cytotoxic limonoids from the stem bark of *Chisocheton pentandrus* (Blanco) Merr. Phytochemistry Letters 35: 63–67.

Xu, M., McCanna, D.J., and Sivak, J.G. 2015. Use the viability reagent PrestoBlue in comparison with alamarBlue and MTT to assess the viability of human corneal epithelial cells. Journal of Pharmacological and Toxicological Methods. 71: 1–7.

Zhao, Y., Jia, Z., and Yang, L. 1994. Sinapyl alcohol derivatives and other constituents from *Ligularia nelumbifolia*. Phytochemistry. 37: 1149-1152.

Zohora, FT., Islam, SN., Khan, S. A., Hasan, C. M. and Ahsan, M. 2019. Antioxidant, cytotoxic, thrombolytic and antimicrobial activity of *Zanthoxylum rhetsa* root bark with two isolated quinolone alkaloids. Pharmacology & Pharmacy. 10: 137-145.

Zou, H.B., Dong, S.Y., Zhou, C.X., Hu, L.H., Wu, Y.H., Li, H.B., Gong, J.X., Sun, L.L., Wu, X.M., et al. 2006. Design, synthesis, and SAR analysis of cytotoxic sinapyl alcohol derivatives. Bioorganic & Medicinal Chemistry. 14: 2060–2071.

OPEN access freely available online
Chiang Mai University Journal of Natural Sciences [ISSN 16851994]
Chiang Mai University, Thailand.
https://cmuj.cmu.ac.th

Supplement

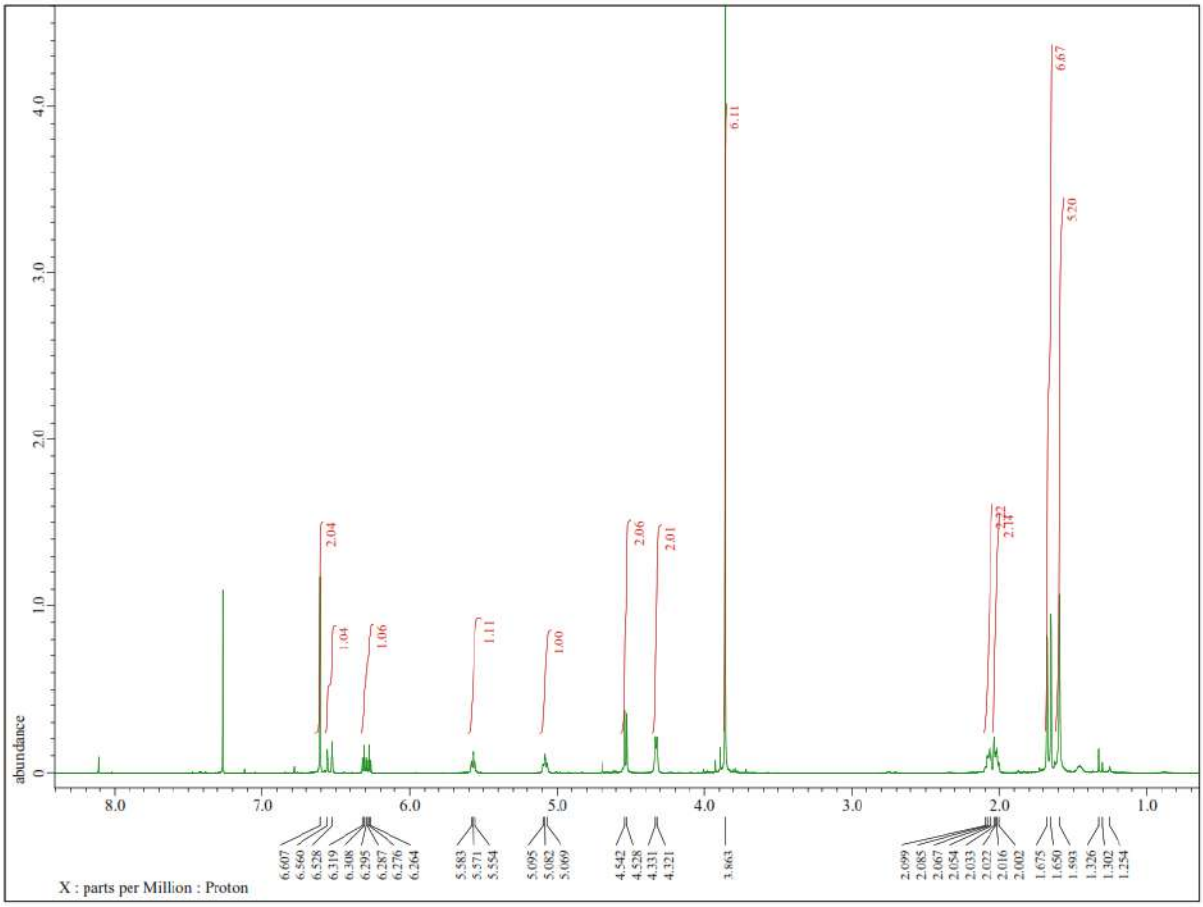

Figure S1. **^{1}H-NMR Spectra of 1 (500 MHz in $CDCl_3$).**

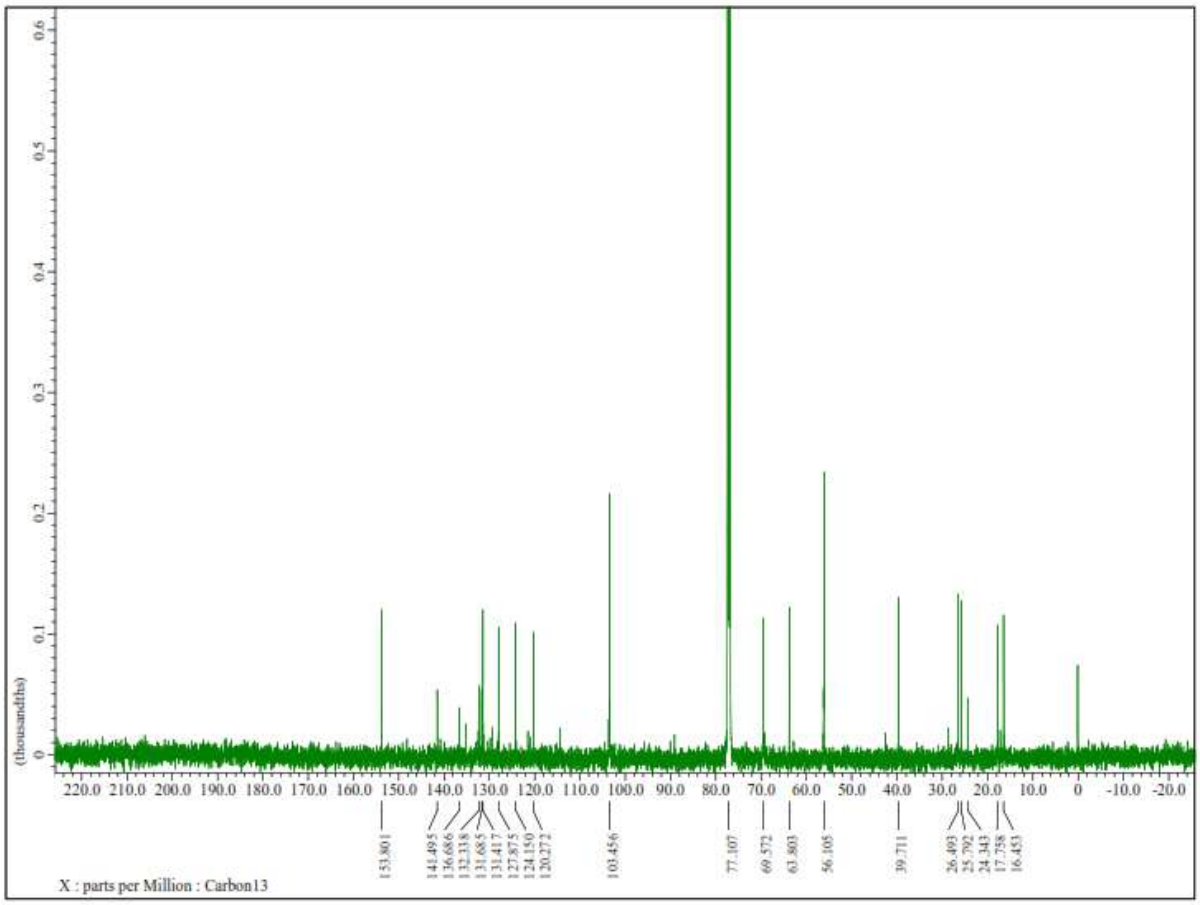

Figure S2. **^{13}C-NMR Spectrum of 1 (125 MHz in $CDCl_3$).**

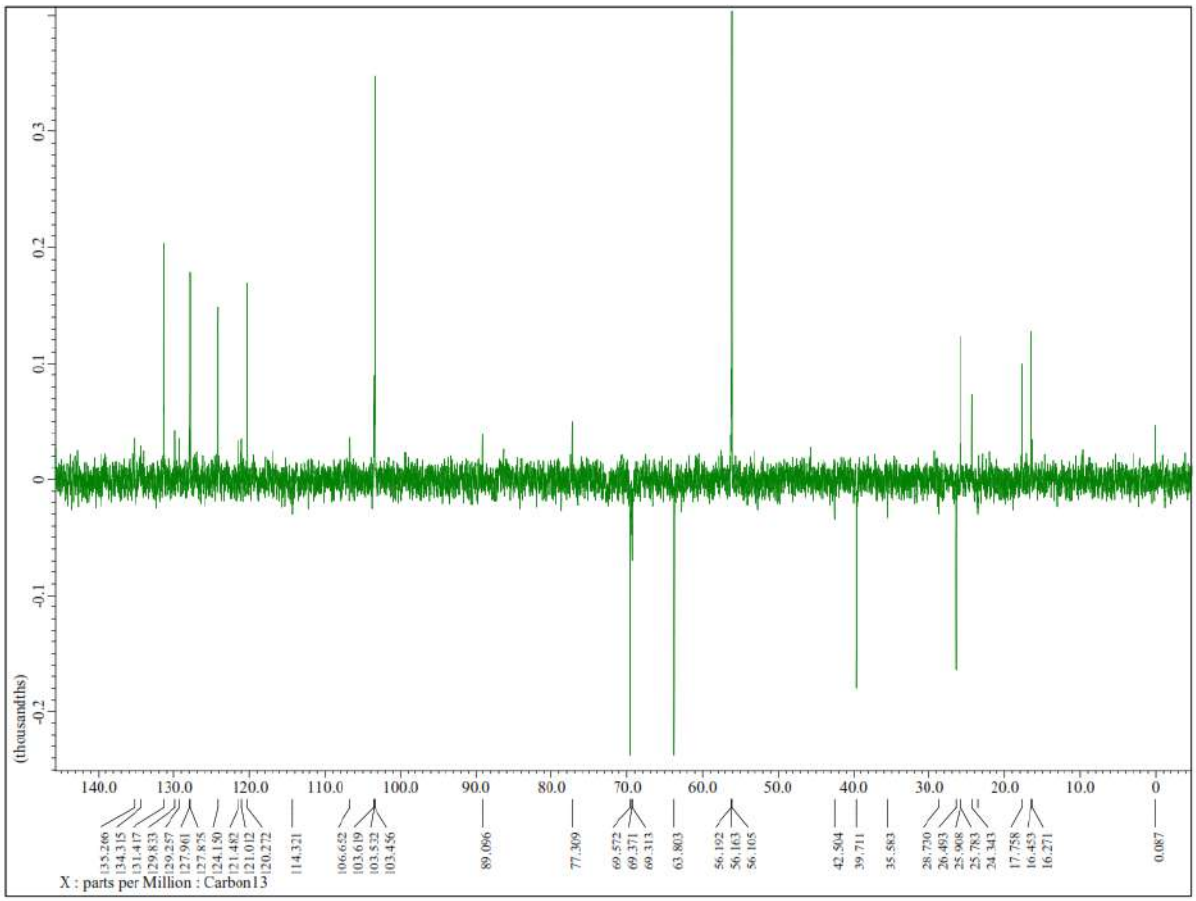

Figure S3. DEPT-135° Spectrum of 1 (125 MHz in $CDCl_3$).

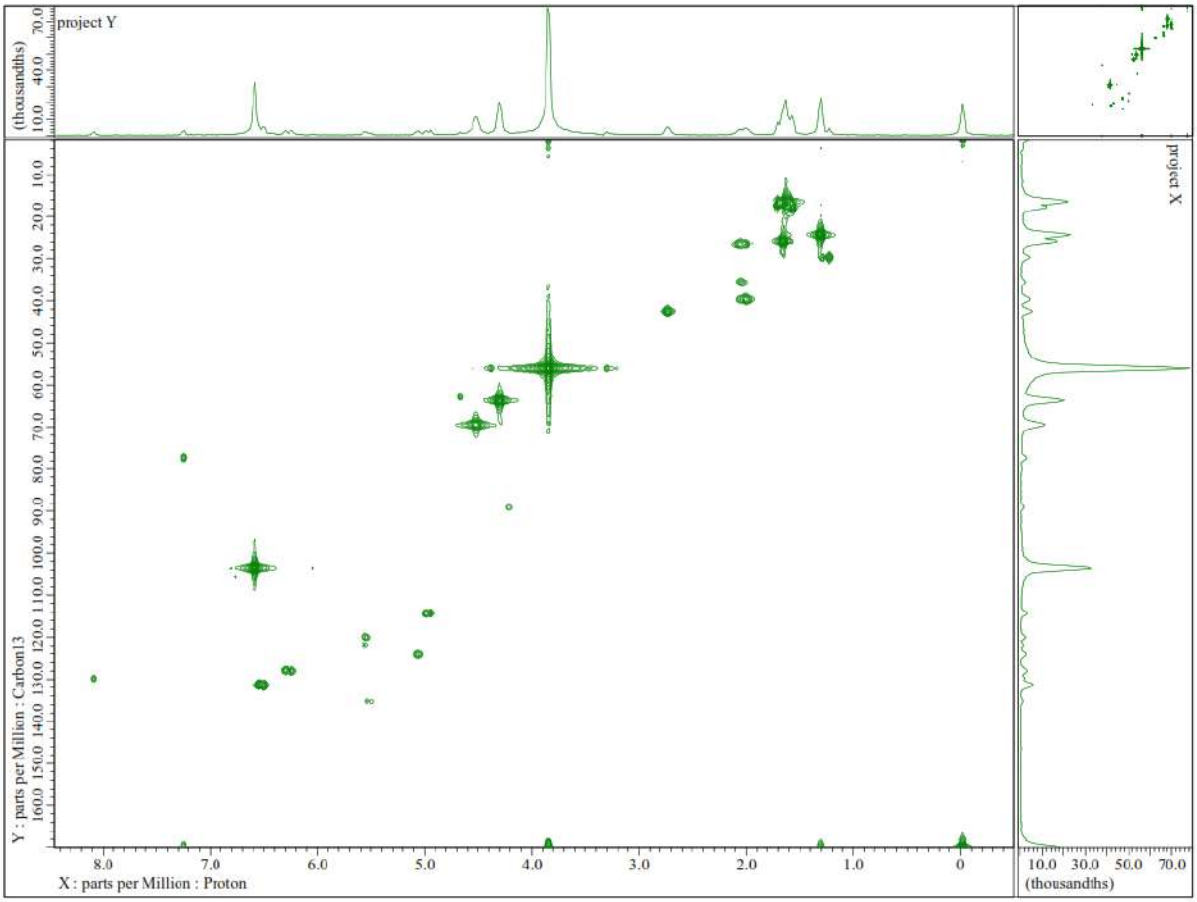

Figure S4. HMQC Spectrum of 1.

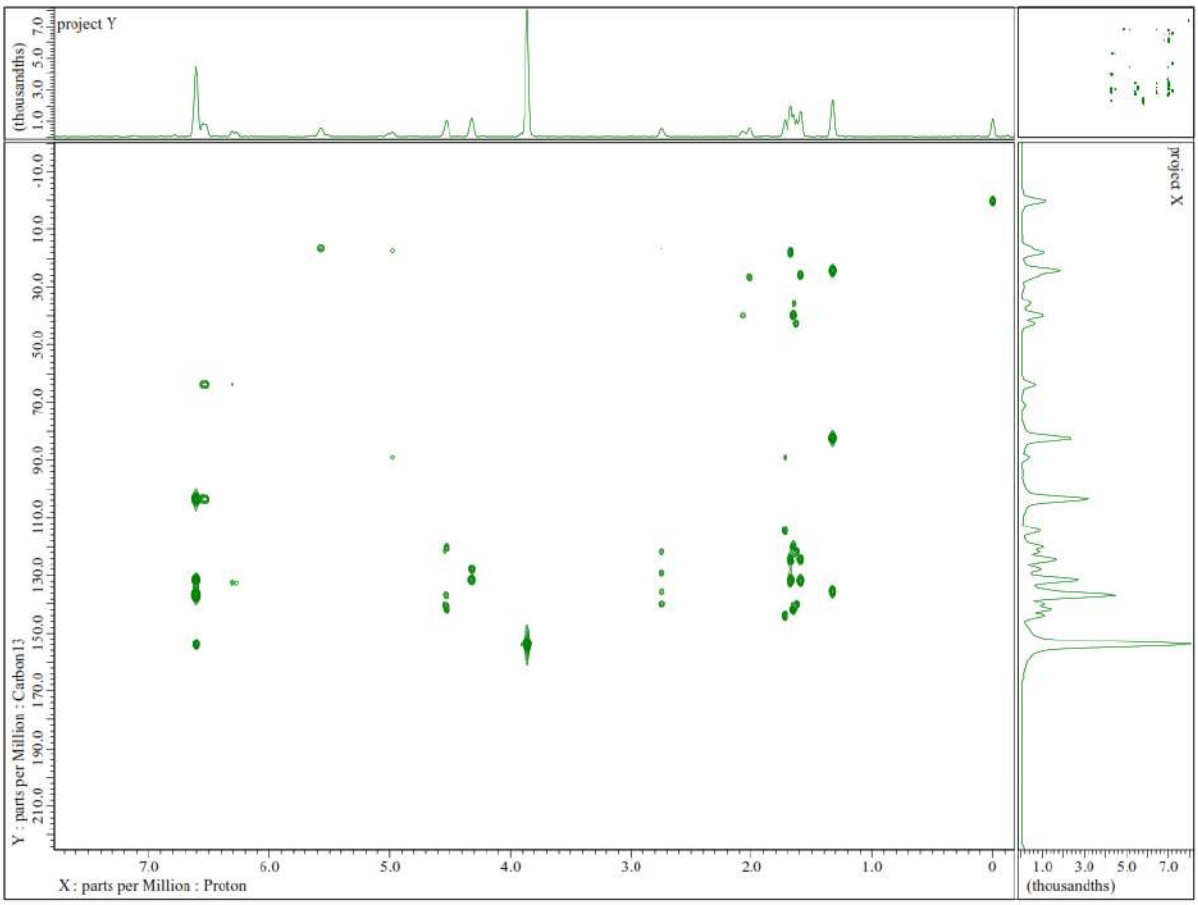

Figure S5. HMBC Spectrum of 1.

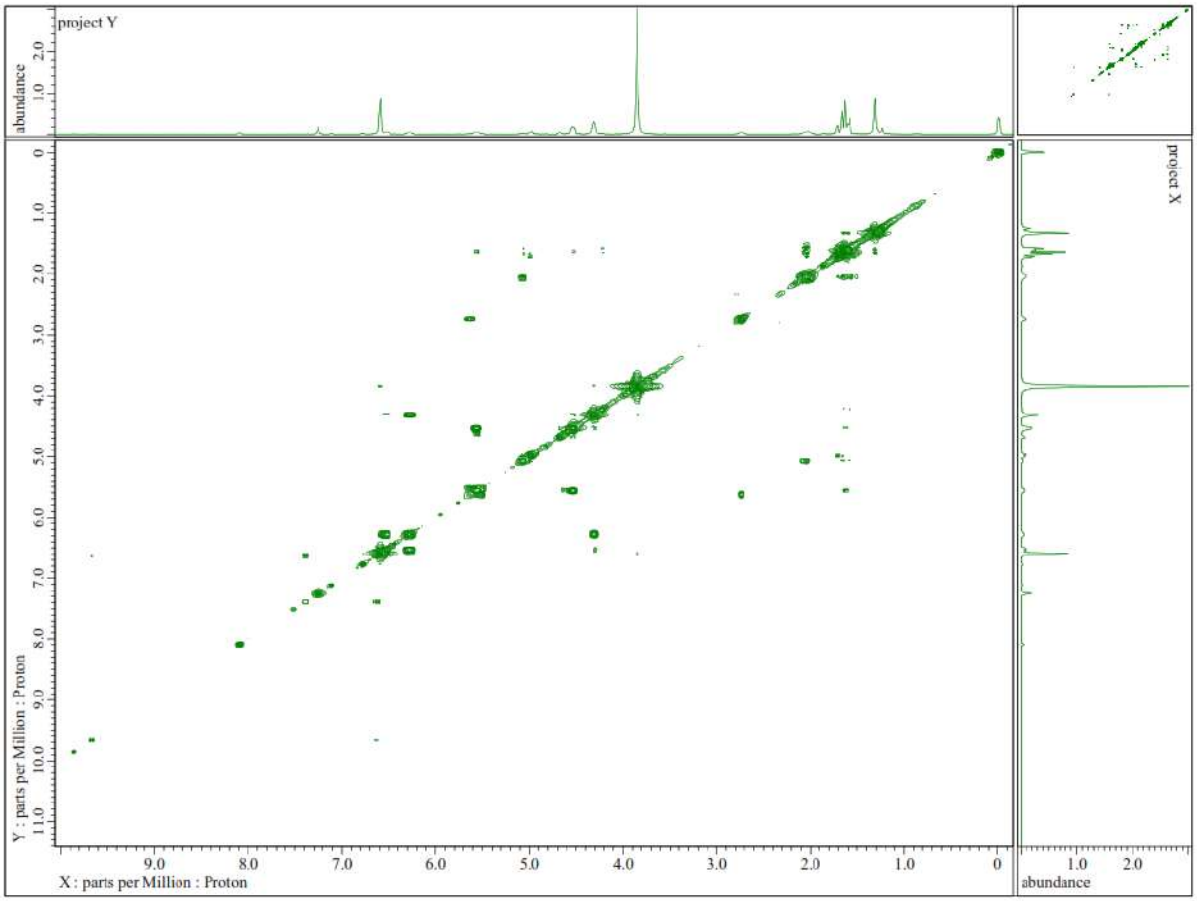

Figure S6. ^{1}H-^{1}H-COSY Spectra of 1.

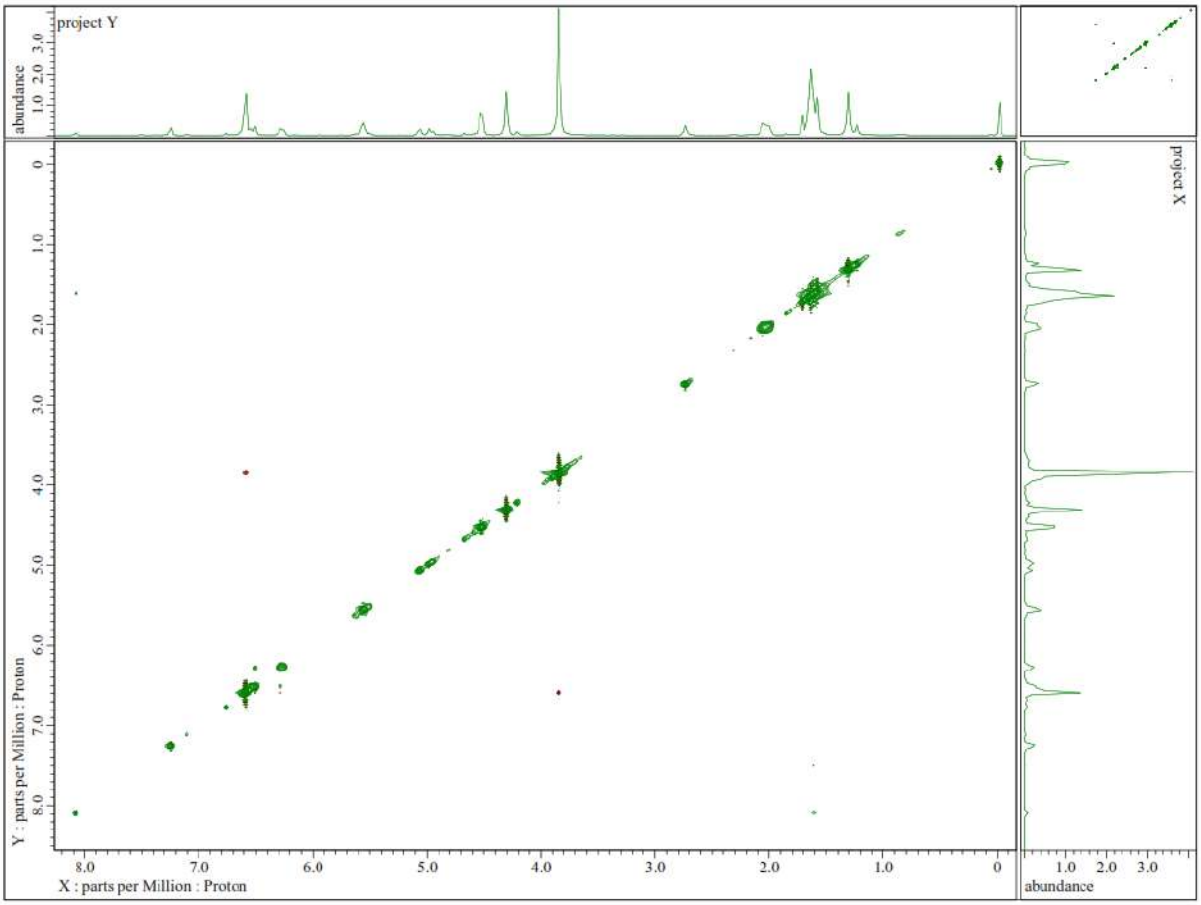

Figure S7. ^{1}H-^{1}H-NOESY Spectrum of 1.

Elemental Composition Report **Page 1**

Single Mass Analysis
Tolerance = 5.0 mDa / DBE: min = -1.5, max = 50.0
Element prediction: Off
Number of isotope peaks used for i-FIT = 3

Monoisotopic Mass, Even Electron Ions
72 formula(e) evaluated with 1 results within limits (all results (up to 1000) for each mass)
Elements Used:
C: 0-500 H: 0-1000 O: 0-200
RCUHI 14 12 (0.221) Cm (1:12)
TOF MS ES+

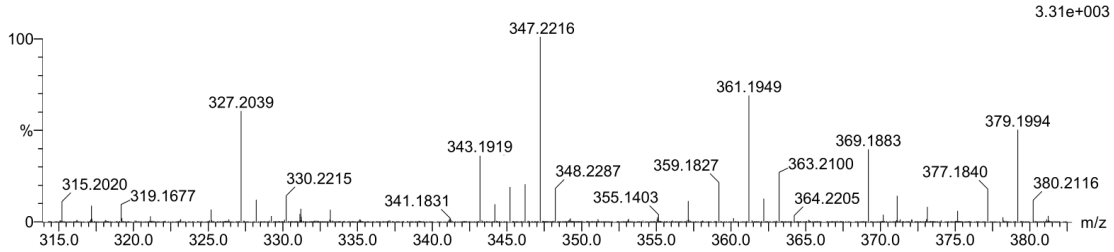

Minimum:				-1.5			
Maximum:		5.0	10.0	50.0			
Mass	Calc. Mass	mDa	PPM	DBE	i-FIT	i-FIT (Norm)	Formula
347.2216	347.2222	-0.6	-1.7	6.5	187.2	0.0	C21 H31 O4

Figure S8. HR-ESI-TOFMS Spectrum of 1.

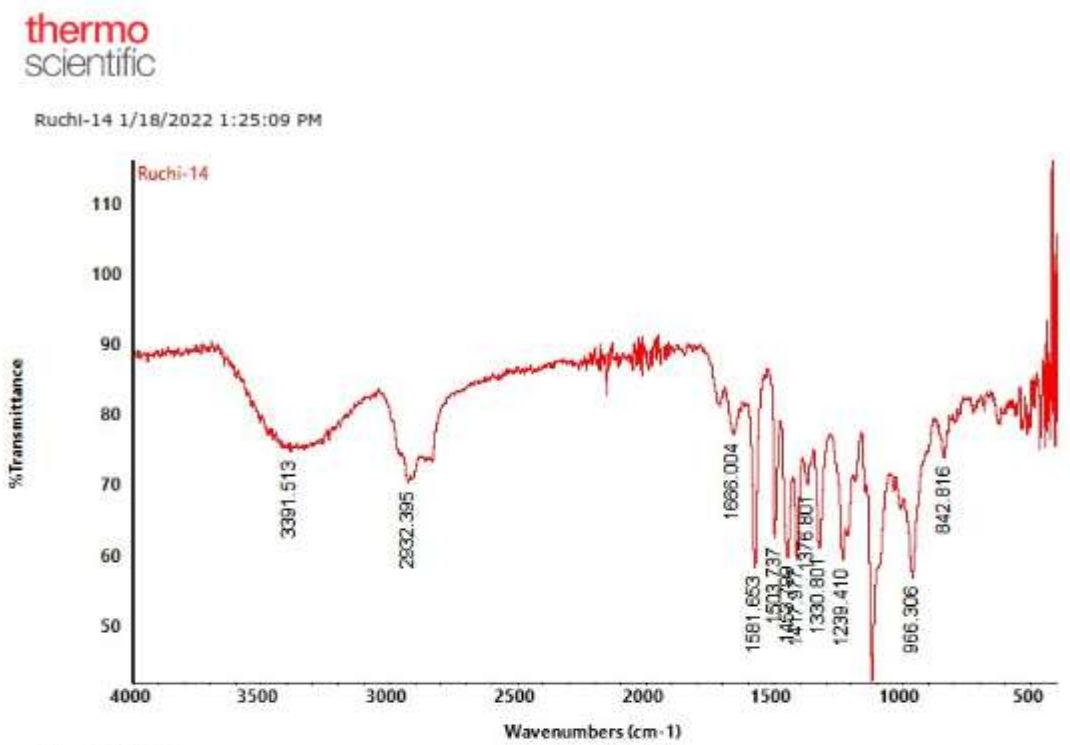

Title: Ruchi-14
Number of sample scans: 16
Number of background scans: 16
Instrument Serial: BDM1910155
Smart Accy: V67654
Model: Summit
Source: IR
Detector: DTGS KBr
Smart Accessory Title: Everest ATR
Smart Accessory ID: V67654
Crystal type: : Diamond
Beamsplitter: KBr
Sample spacing: 1.0
Digitizer bits: 24
Optical velocity: 0.4747
Aperture: 100.0
Sample gain: 1.0
High pass filter: 1.0
Low pass filter: 11000.0
Comments: None

Regions:

Region 1: 3702.54-610.95
Threshold: 78.83
Sensitivity: 41.00

Position	Intensity
842.82	73.58
966.31	56.65
1124.84	41.71
1239.41	59.03
1330.80	60.78
1376.80	69.74
1417.98	59.11
1453.80	59.45
1503.74	62.27
1581.65	57.99
1666.00	76.90
2932.40	70.06
3391.51	74.39

Figure S9. FTIR Spectrum of 1.

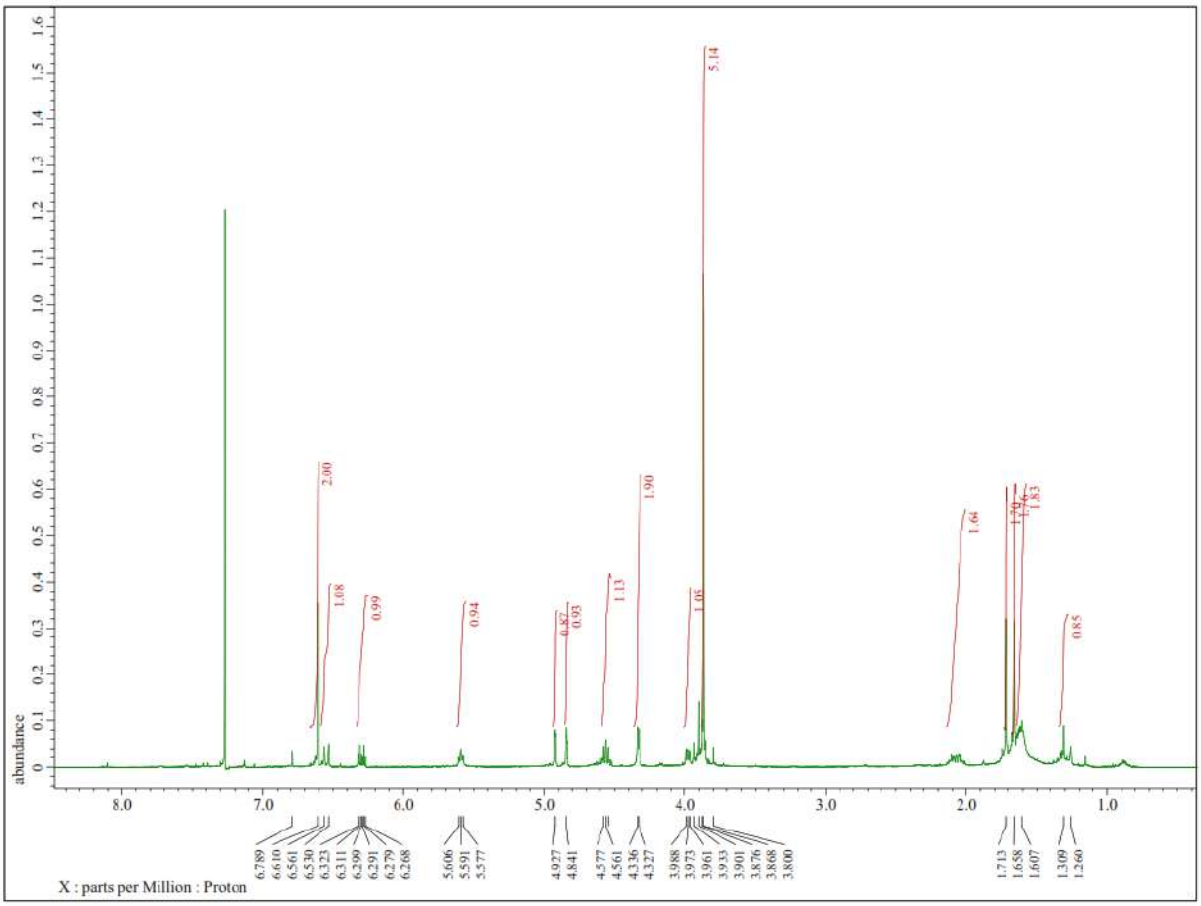

Figure S10. **^{1}H-NMR Spectra of 2 (500 MHz in $CDCl_3$).**

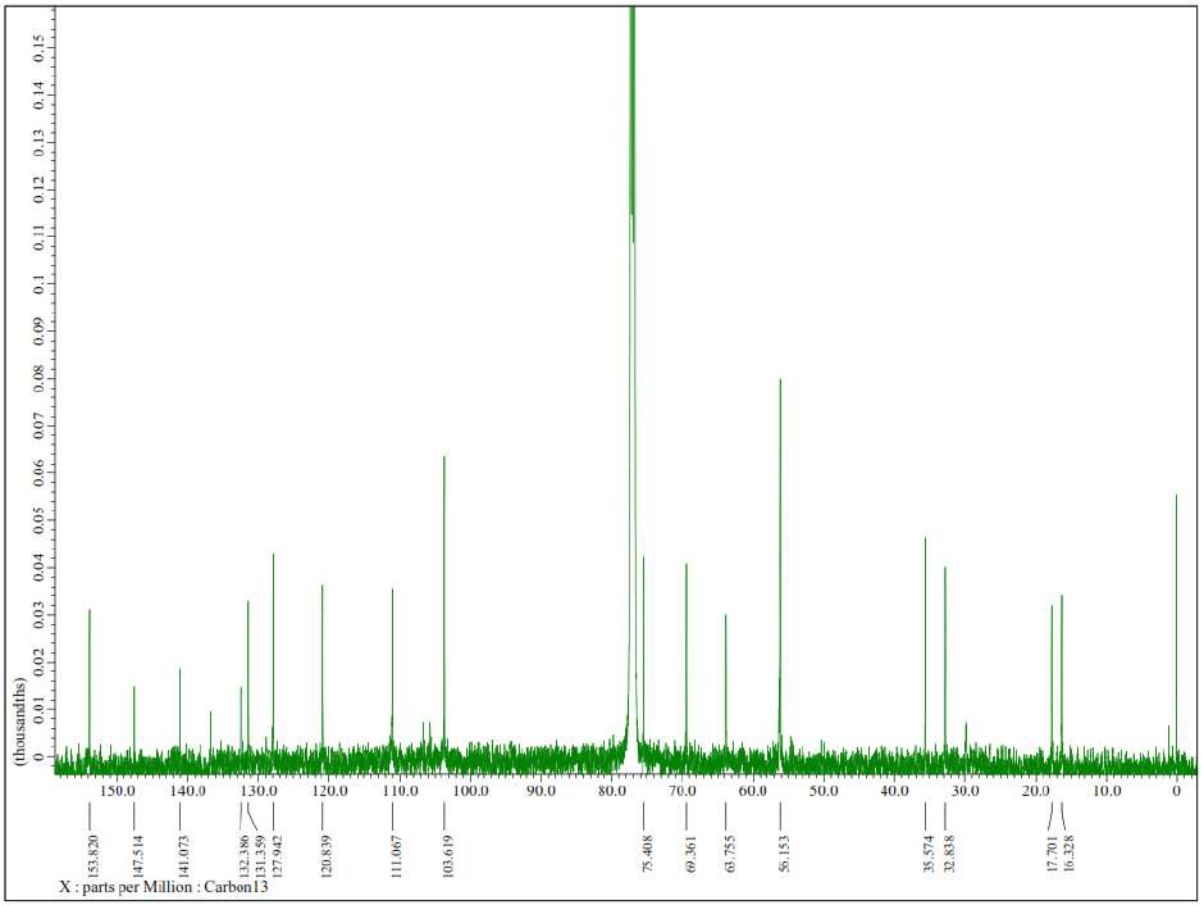

Figure S11. **^{13}C-NMR Spectrum of 2 (125 MHz in $CDCl_3$).**

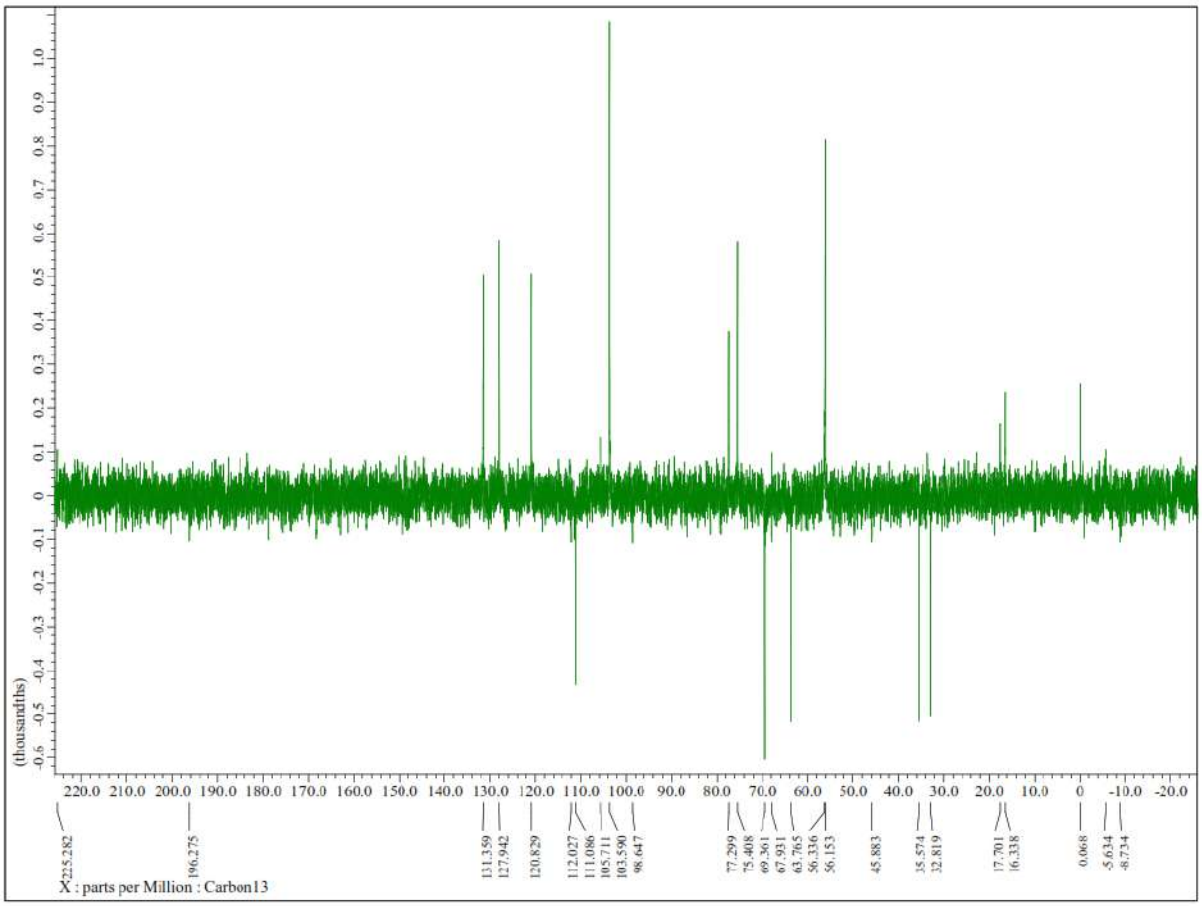

Figure S12. DEPT-135° Spectrum of 2(125 MHz in $CDCl_3$).

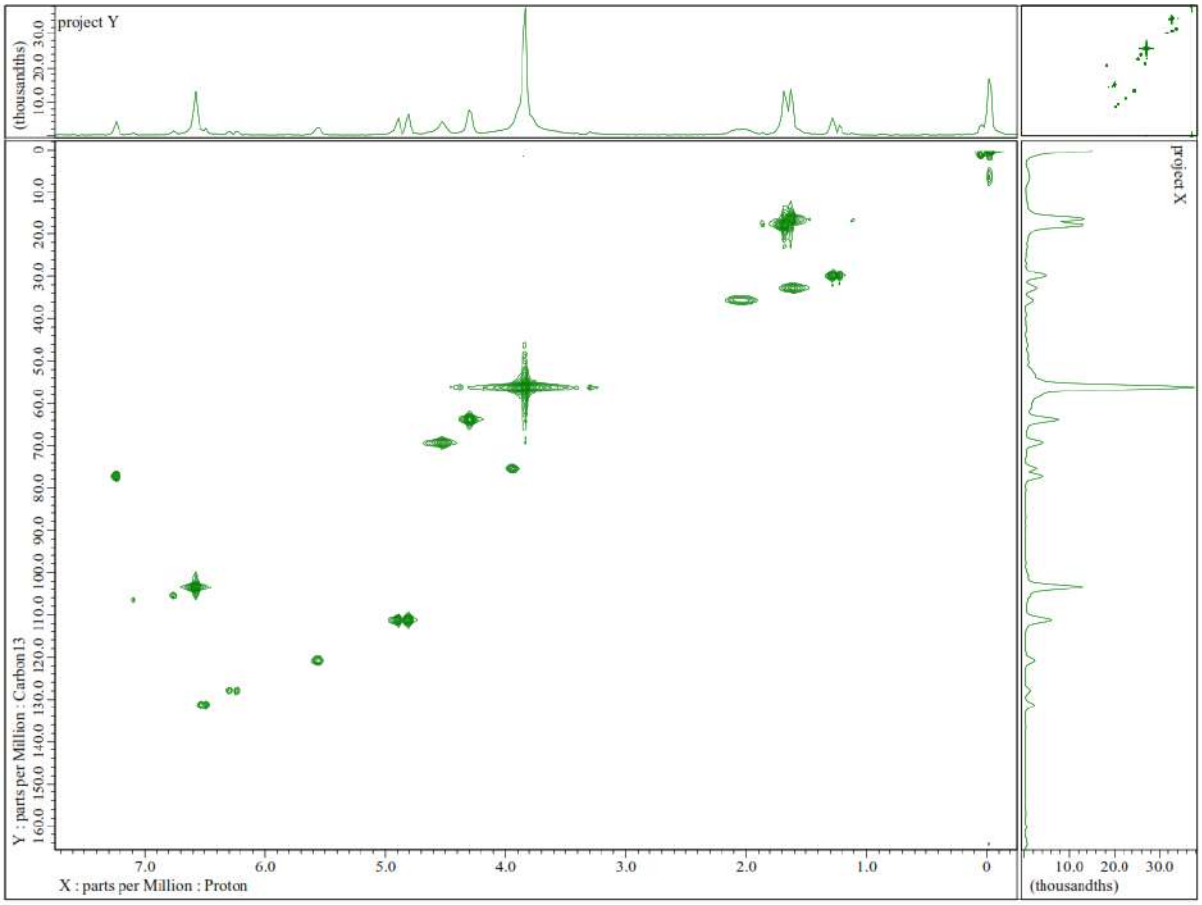

Figure S13. HMQC Spectrum of 2.

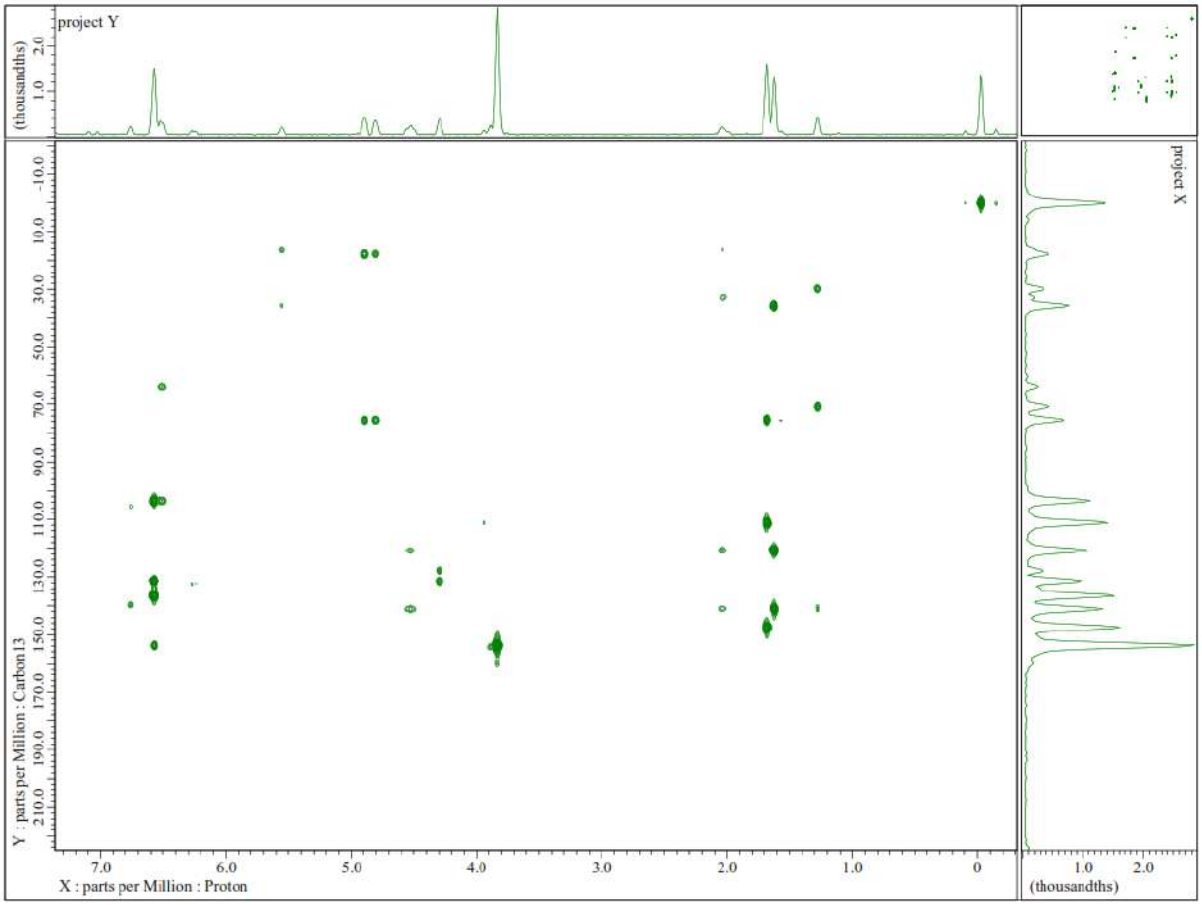

Figure S14. HMBC Spectrum of 2.

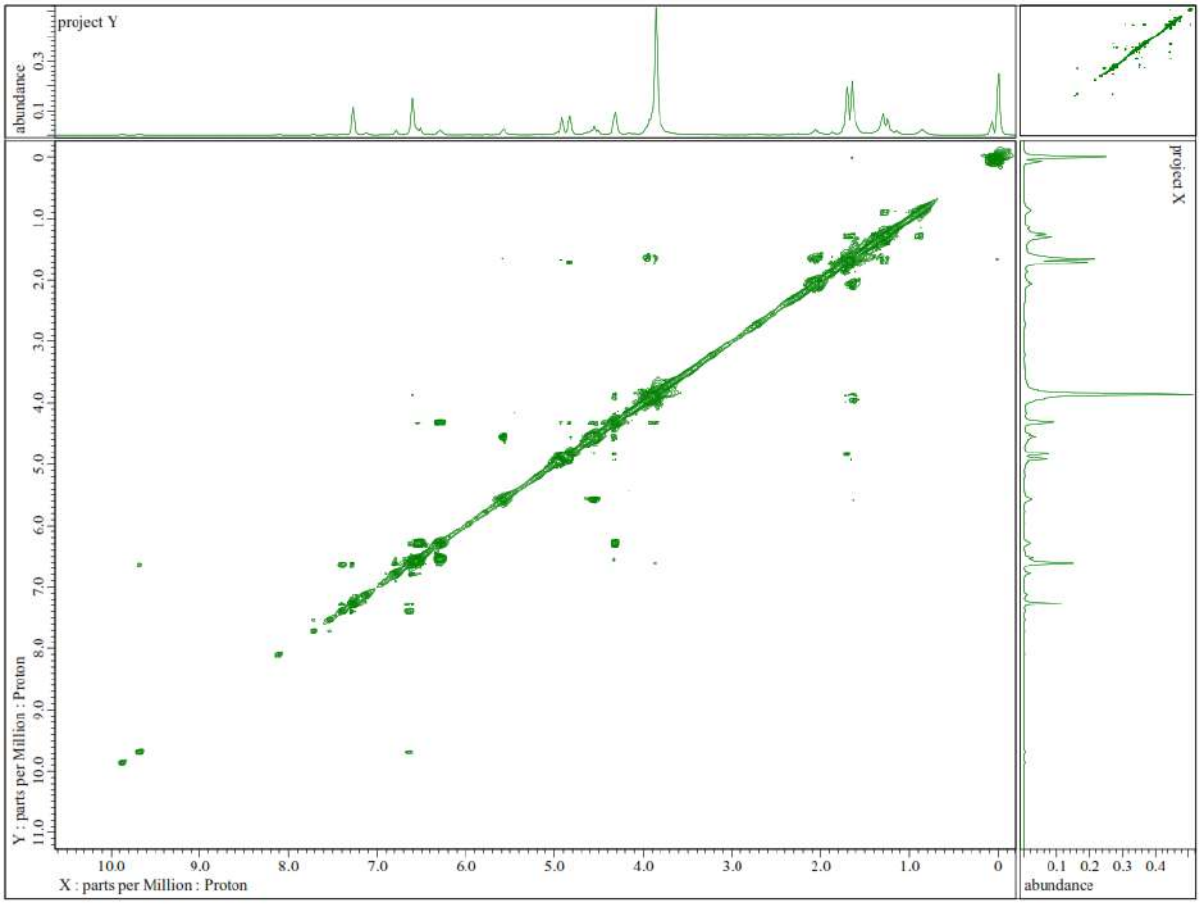

Figure S15. **^{1}H-^{1}H-COSY Spectra of 2.**

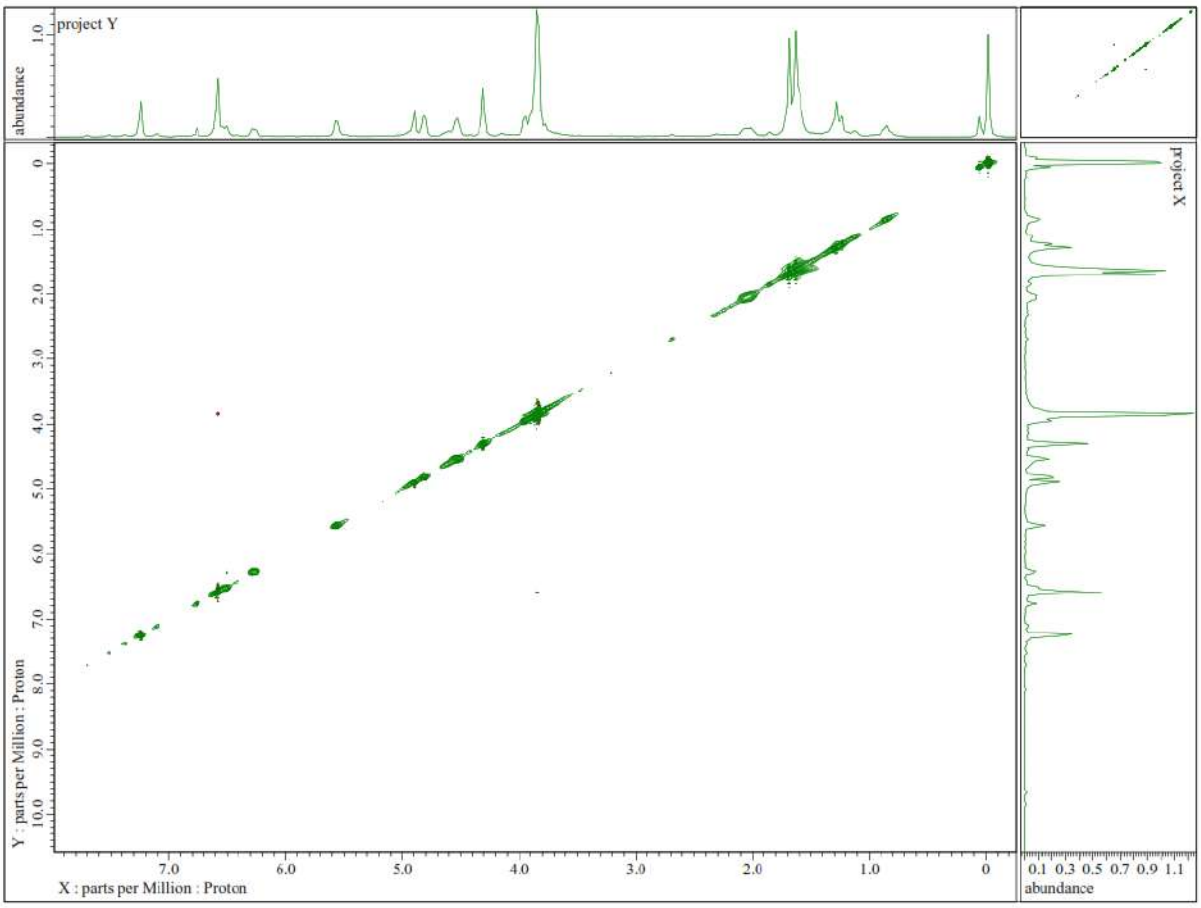

Figure S16. ^{1}**H-**^{1}**H-NOESY Spectrum of 2.**

Elemental Composition Report **Page 1**

Single Mass Analysis
Tolerance = 5.0 mDa / DBE: min = -1.5, max = 50.0
Element prediction: Off
Number of isotope peaks used for i-FIT = 3

Monoisotopic Mass, Even Electron Ions
150 formula(e) evaluated with 3 results within limits (all results (up to 1000) for each mass)
Elements Used:
C: 0-500 H: 0-1000 O: 0-200 Na: 0-1

RUCI 17 7 (0.136) Cm (3:8)
TOF MS ES+

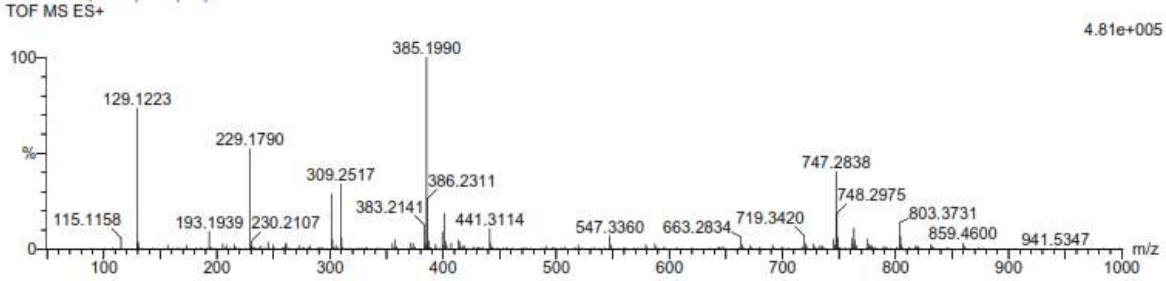

Minimum:				-1.5			
Maximum:		5.0	10.0	50.0			
Mass	Calc. Mass	mDa	PPM	DBE	i-FIT	i-FIT (Norm)	Formula
385.1990	385.1991	-0.1	-0.3	6.5	211.7	9.7	C21 H30 O5 Na
	385.2015	-2.5	-6.5	9.5	202.0	0.0	C23 H29 O5
	385.1956	3.4	8.8	18.5	216.0	14.0	C30 H25

Figure S17. HR-ESI-TOFMS Spectrum of 2.

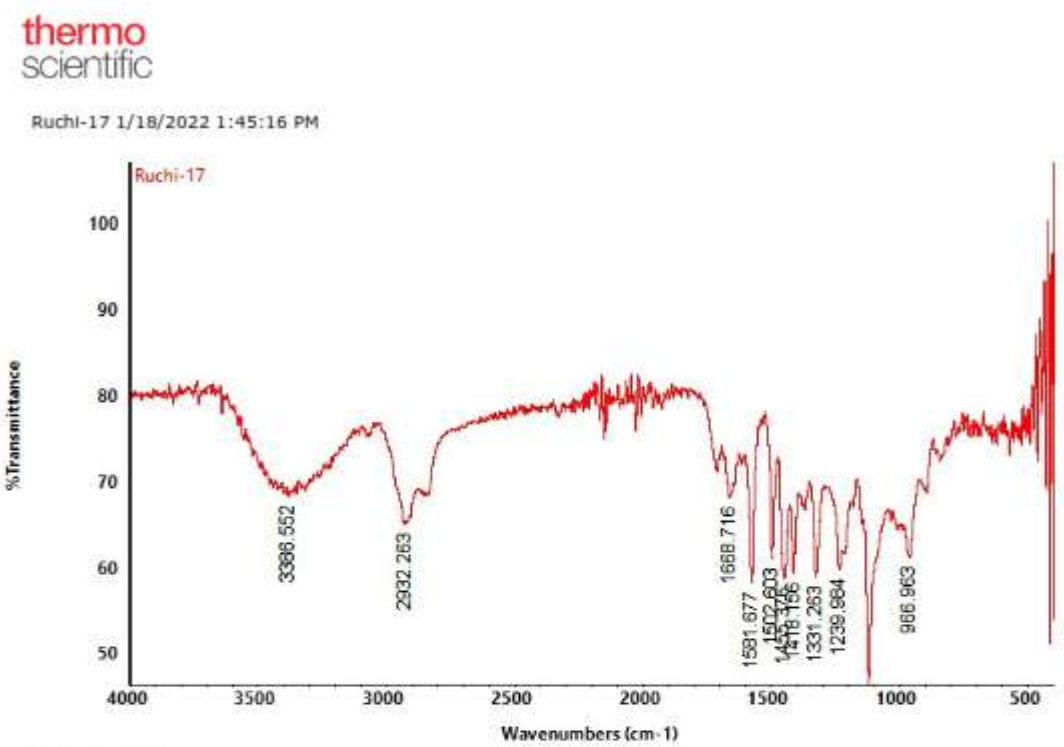

Title: Ruchi-17
Number of sample scans: 16
Number of background scans: 16
Instrument Serial: BDM1910155
Smart Accy: V67654
Model: Summit
Source: IR
Detector: DTGS KBr
Smart Accessory Title: Everest ATR
Smart Accessory ID: V67654
Crystal type: : Diamond
Beamsplitter: KBr
Sample spacing: 1.0
Digitizer bits: 24
Optical velocity: 0.4747
Aperture: 100.0
Sample gain: 1.0
High pass filter: 1.0
Low pass filter: 11000.0
Comments: None

Regions:

Region 1: 4000.12-658.49
Threshold: 70.47
Sensitivity: 41.00

Position	Intensity
966.96	60.92
1125.73	46.26
1239.98	59.54
1331.26	58.83
1418.16	59.08
1455.38	58.54
1502.60	60.82
1581.68	58.13
1668.72	67.89
2932.26	64.92
3386.55	68.17

Figure S18. FTIR Spectrum of 2.

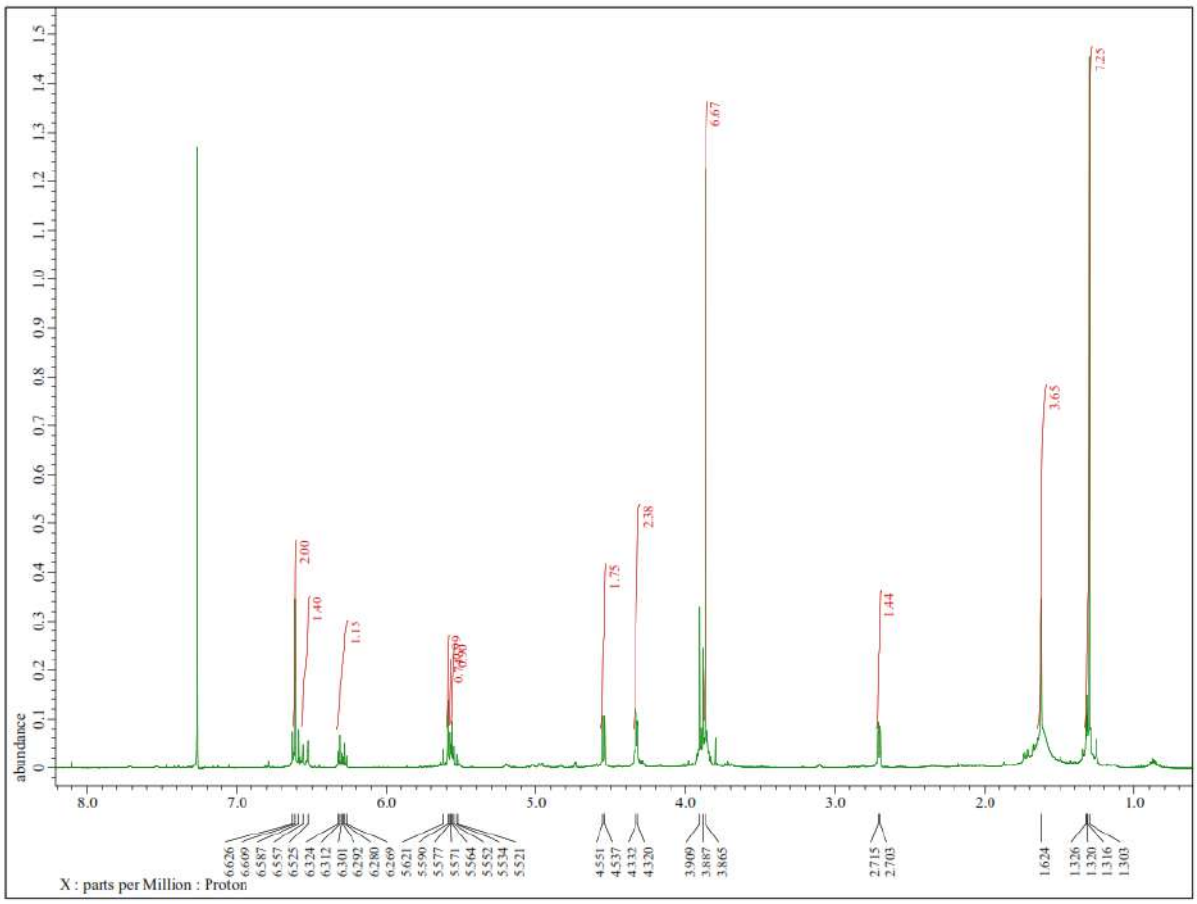

Figure S19. **^{1}H-NMR Spectra of 3 (500 MHz in $CDCl_3$).**

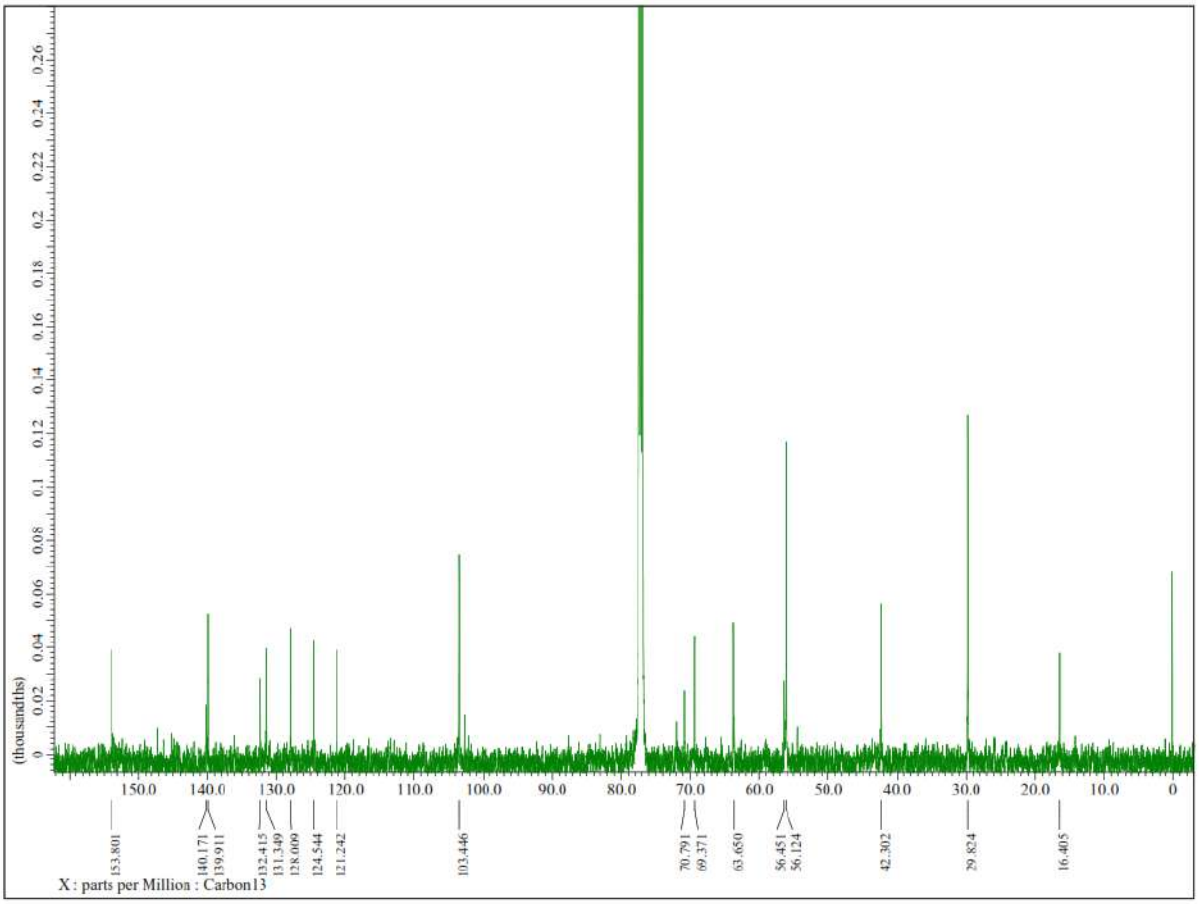

Figure S20. ^{13}**C-NMR Spectrum of 3 (125 MHz in** $CDCl_3$**).**

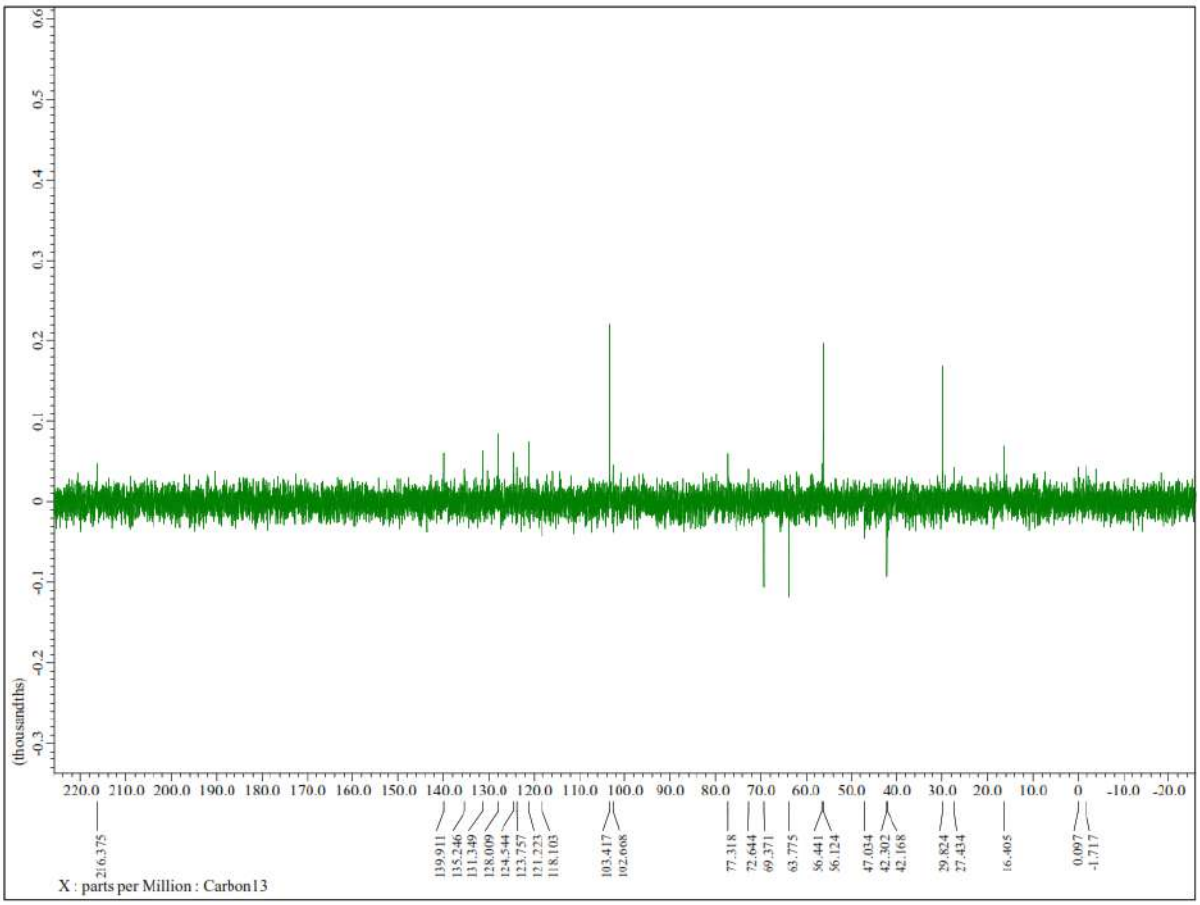

Figure S21. DEPT-135° Spectrum of 3 (125 MHz in $CDCl_3$).

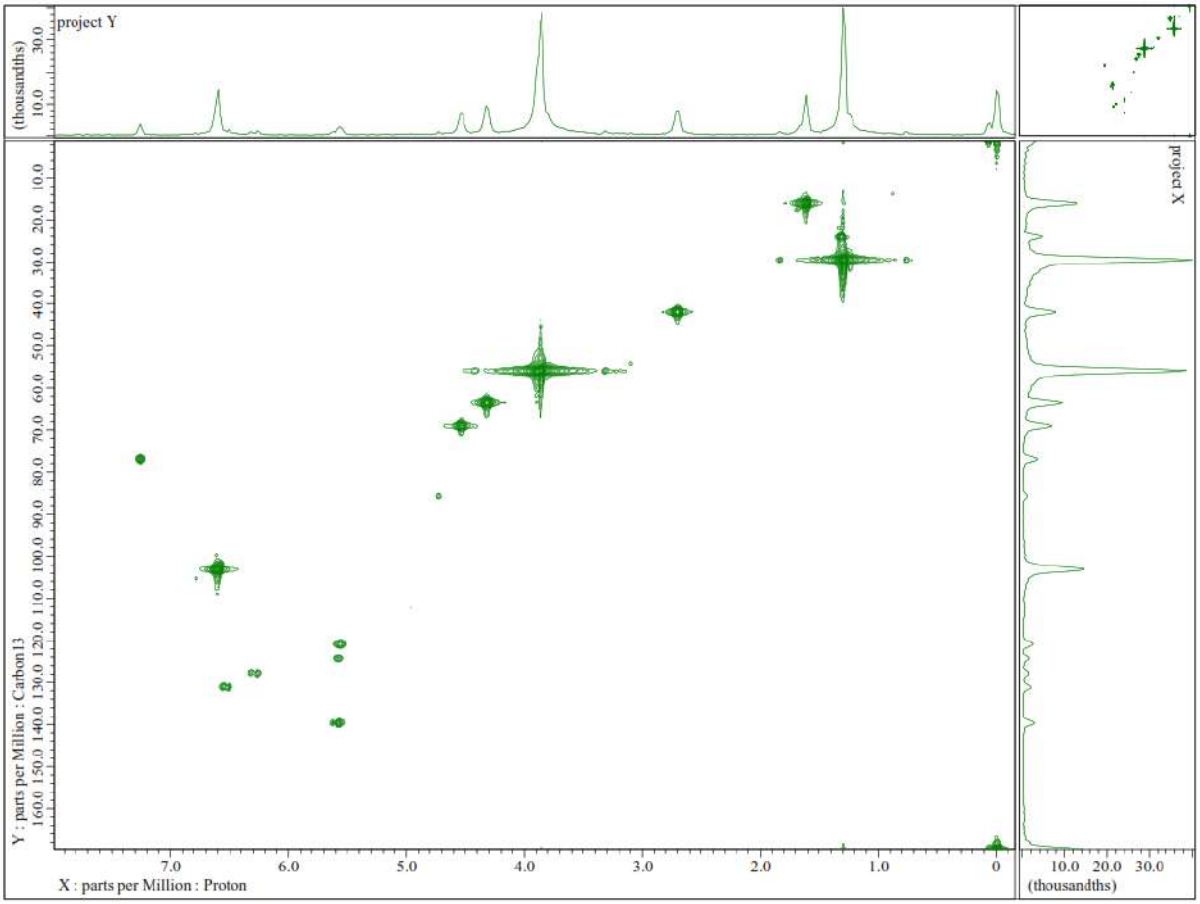

Figure S22. HMQC Spectrum of 3.

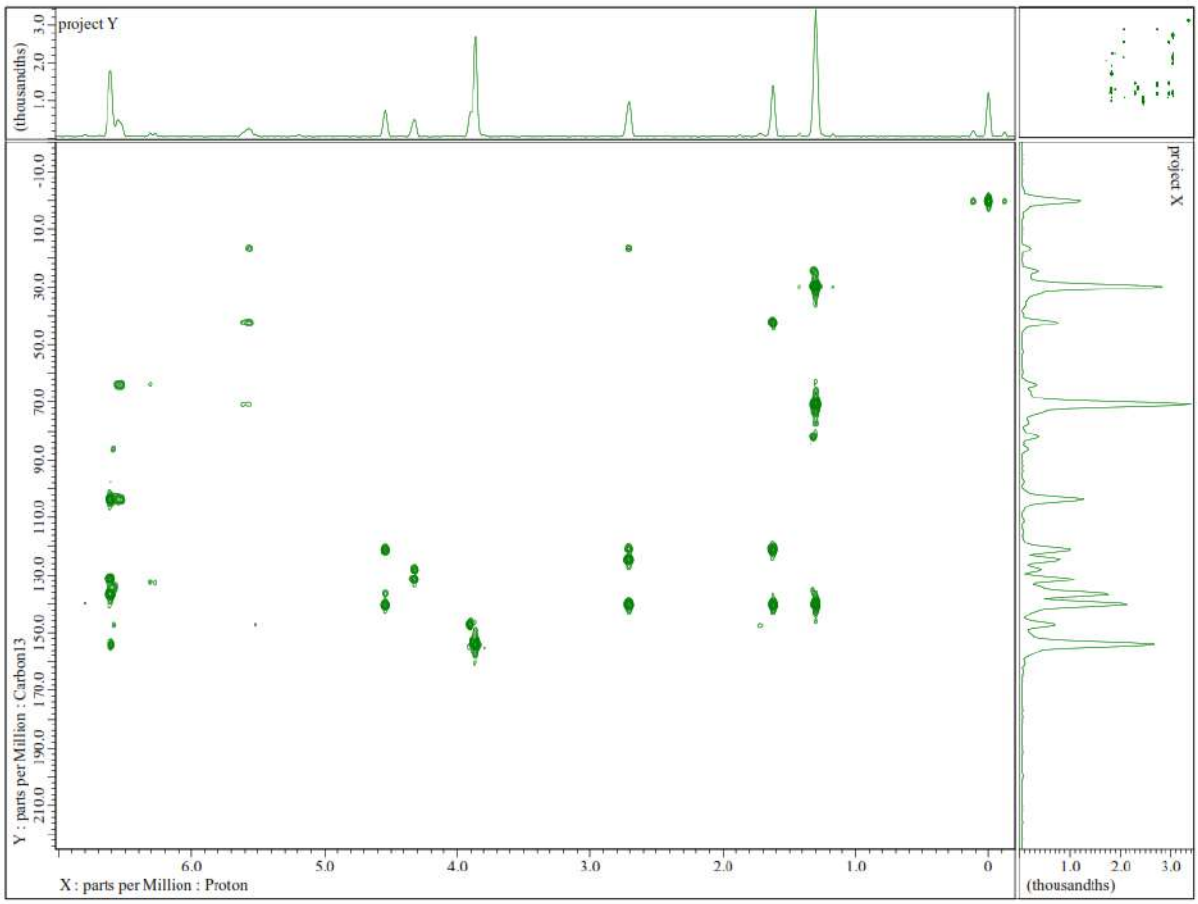

Figure S23. HMBC Spectrum of 3.

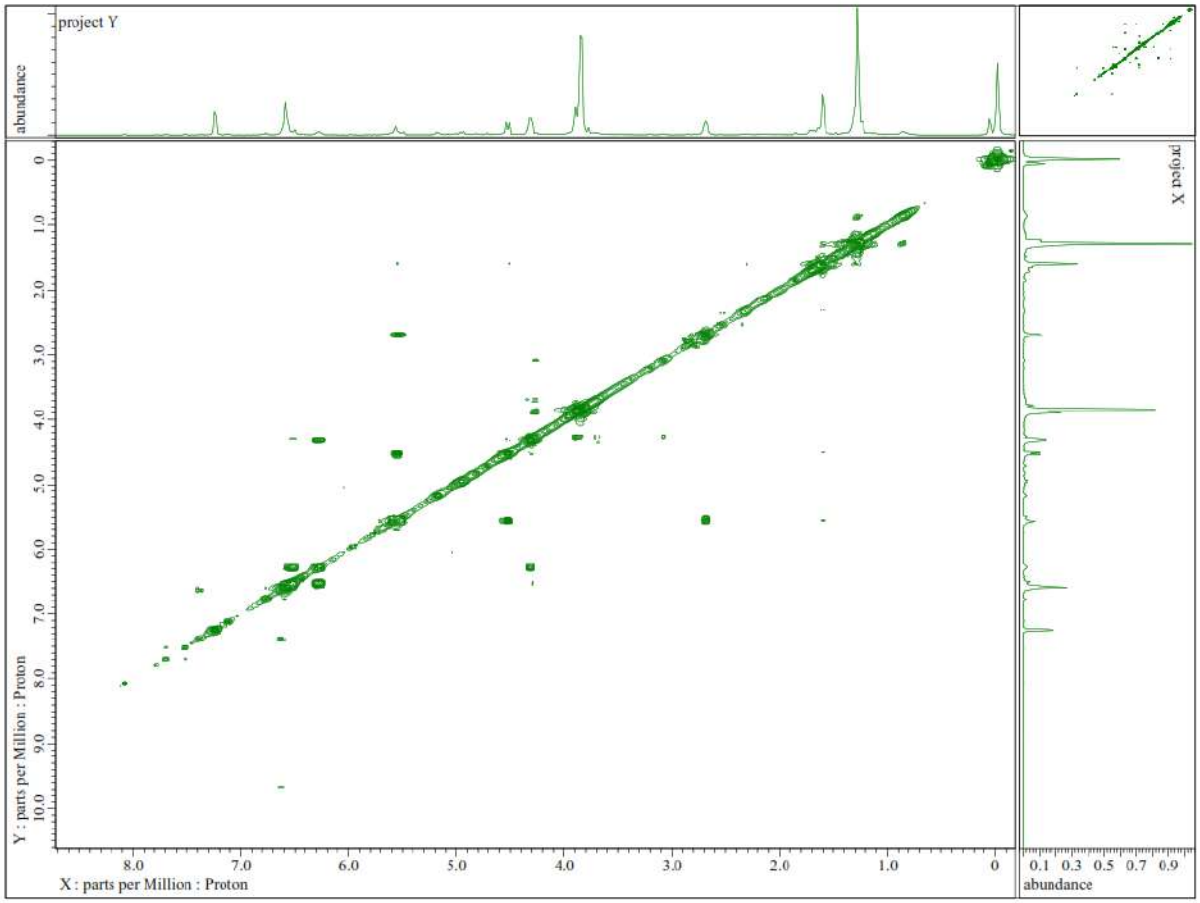

Figure S24. ^{1}H-^{1}H-COSY Spectra of 3.

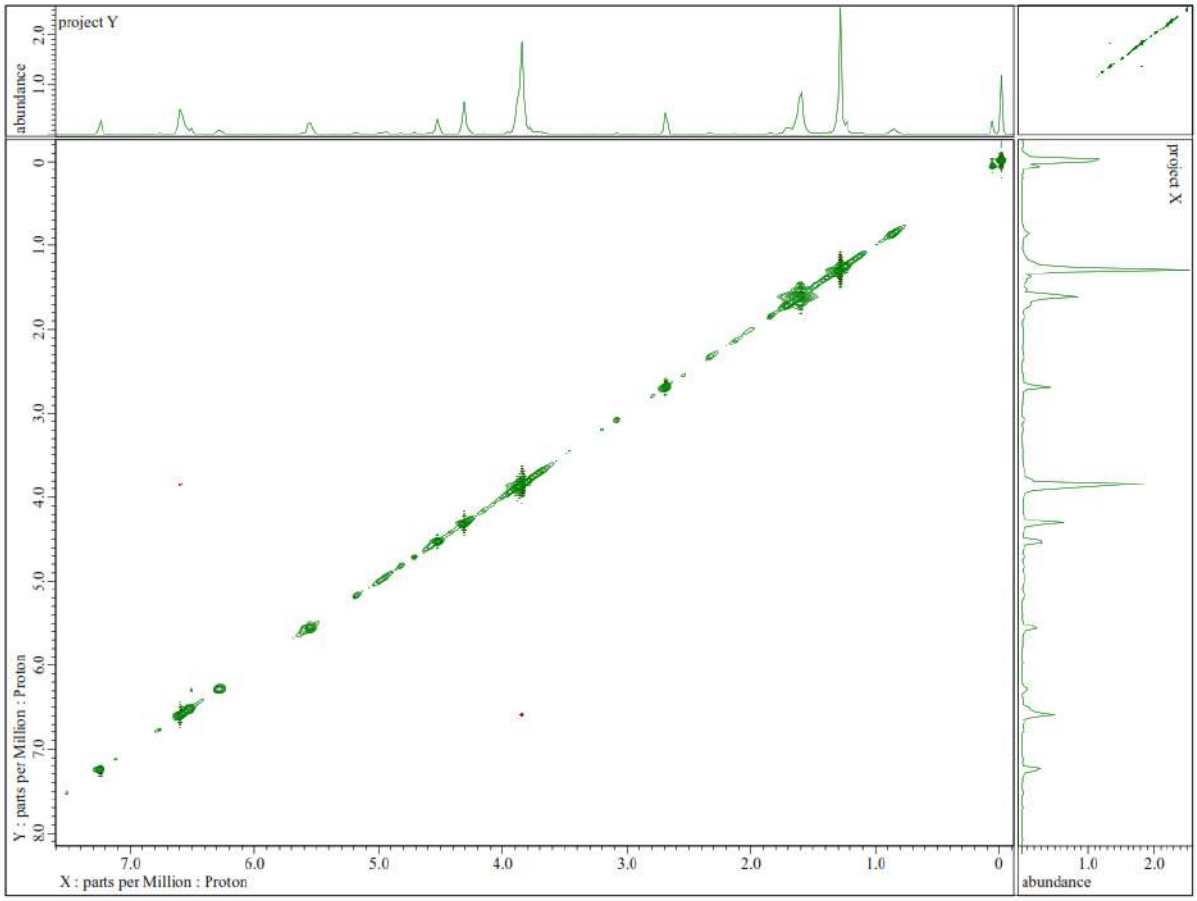

Figure S25. ^{1}**H-**^{1}**H-NOESY Spectrum of 3.**

Single Mass Analysis
Tolerance = 5.0 mDa / DBE: min = -1.5, max = 50.0
Element prediction: Off
Number of isotope peaks used for i-FIT = 3

Monoisotopic Mass, Even Electron Ions
150 formula(e) evaluated with 2 results within limits (all results (up to 1000) for each mass)
Elements Used:
C: 0-500 H: 0-1000 O: 0-200 Na: 0-1

RUCI 18 8 (0.153) Cm (8)
TOF MS ES+

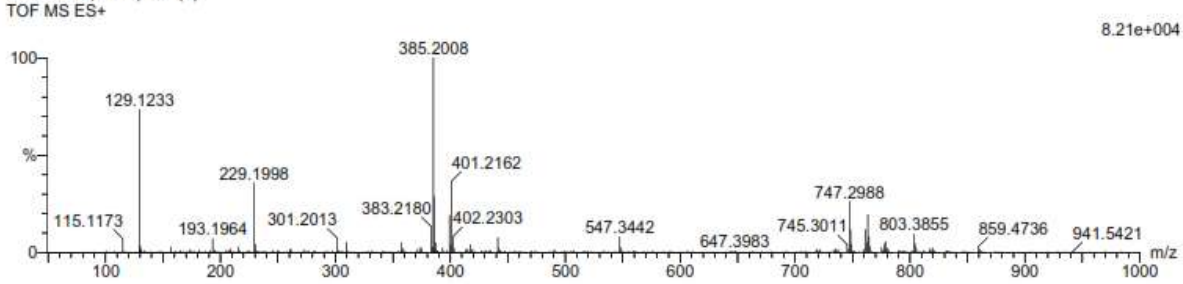

Minimum:				-1.5			
Maximum:		5.0	10.0	50.0			
Mass	Calc. Mass	mDa	PPM	DBE	i-FIT	i-FIT (Norm)	Formula
385.2008	385.2015	-0.7	-1.8	9.5	111.9	0.1	C23 H29 O5
	385.1991	1.7	4.4	6.5	114.6	2.8	C21 H30 O5 Na

Figure S26. HR-ESI-TOFMS Spectrum of 3.

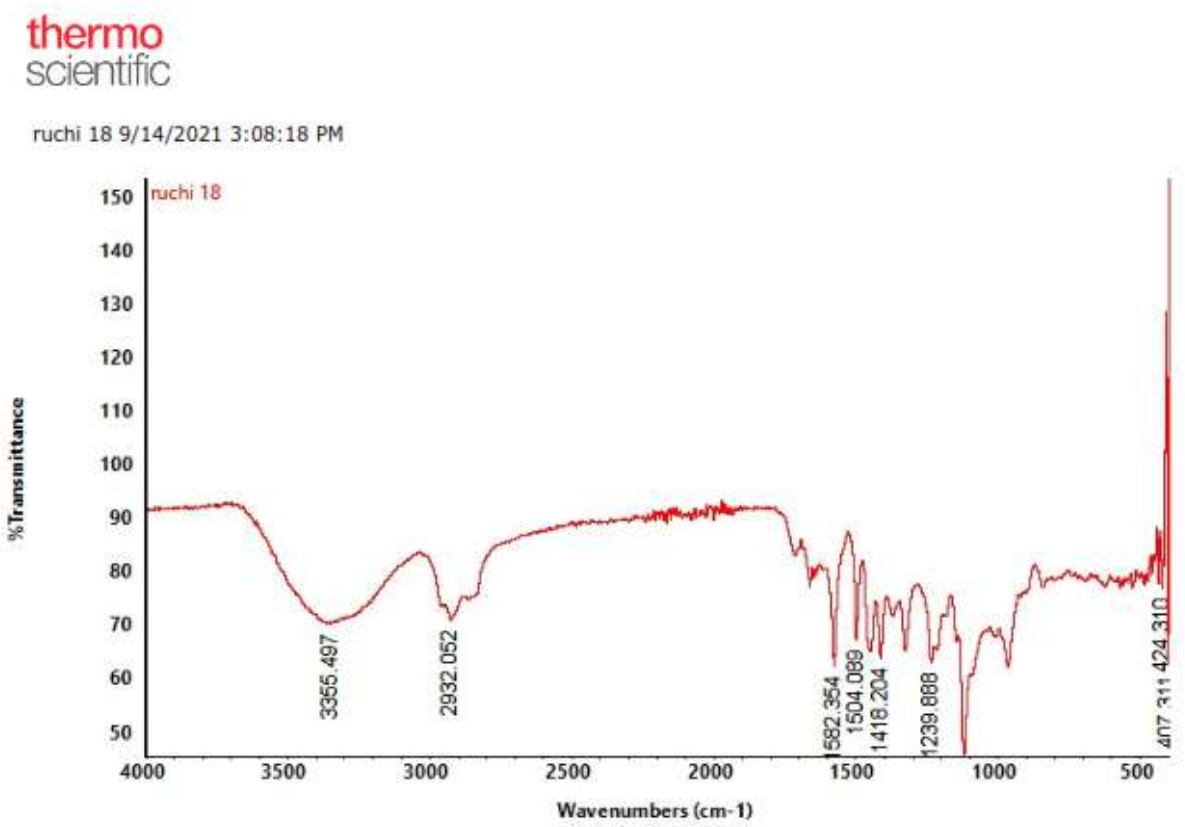

Title: ruchi 18
Number of sample scans: 16
Number of background scans: 16
Instrument Serial: BDM1910155
Smart Accy: V67654
Model: Summit
Source: IR
Detector: DTGS KBr
Smart Accessory Title: Everest ATR
Smart Accessory ID: V67654
Crystal type: : Diamond
Beamsplitter: KBr
Sample spacing: 1.0
Digitizer bits: 24
Optical velocity: 0.4747
Aperture: 100.0
Sample gain: 1.0
High pass filter: 1.0
Low pass filter: 11000.0
Comments: None

Figure S27. FTIR Spectrum of 3.

Concentration	Corrected Absorbance	Target Absorbansi IC50	Konsentrasi Sampel Absorbansi IC50
1000,00	-0,0060	0,3767	54,18
500,00	0,0014		
250,00	0,0053		
125,00	0,0146		
62,50	0,2787		
31,25	0,6296		
15,63	0,7258		
7,81	0,7284		

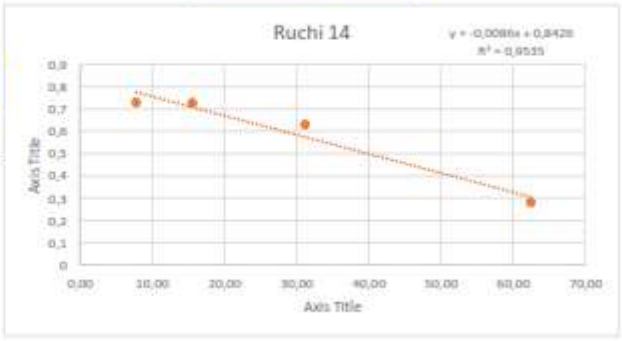

Figure S28. Cytotoxic activity of 1 against MCF-7 breast cancer cells line.

Concentration	Corrected Absorbance	Target Absorbansi IC50	Konsentrasi Sampel Absorbansi IC50
1000,00	-0,0041	0,3733	92,51
500,00	0,0034		
250,00	0,0150		
125,00	0,1894		
62,50	0,5613		
31,25	0,7201		
15,63	0,7320		
7,81	0,7337		

Figure S29.Cytotoxic activity of 2 against MCF-7 breast cancer cells line.

Concentration	Corrected Absorbance	Target Absorbansi IC50	Konsentrasi Sampel Absorbansi IC50
1000,00	0,0011	0,3796	60,21
500,00	0,0061		
250,00	0,0105		
125,00	0,1100		
62,50	0,3269		
31,25	0,6807		
15,63	0,7360		
7,81	0,7472		

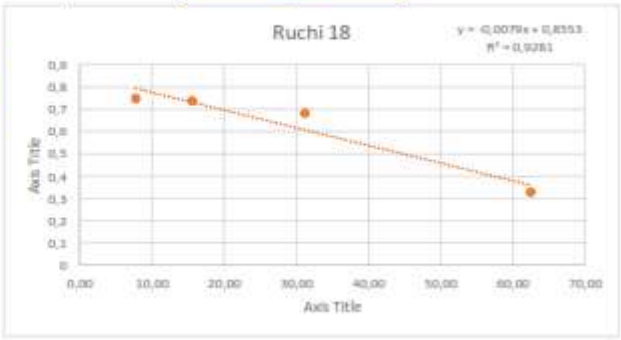

Figure S30. Cytotoxic activity of 3 against MCF-7 breast cancer cells line.